TRENDS IN COASTAL OCEAN CONDITIONS ON O‘AHU, HAWAI‘I’S URBAN SHORES

A THESIS SUBMITTED TO
THE GLOBAL ENVIRONMENTAL SCIENCE
UNDERGRADUATE DIVISION IN PARTIAL FULFILLMENT
OF THE REQUIREMENTS FOR THE DEGREE OF

BACHELOR OF SCIENCE

IN

GLOBAL ENVIRONMENTAL SCIENCE

AUGUST 2020

By
SHAUN A. WRISTON

Thesis Advisor

Margaret Anne McManus, Ph. D.

I certify that I have read this thesis and that, in my opinion, it is satisfactory in scope and quality as a thesis for the degree of Bachelor of Science in Global Environmental Science.

THESIS ADVISOR

_____

Margaret Anne McManus, Ph. D.
Department of Oceanography

For Mom, Dad, Marisa and Han

Acknowledgements

I would like to thank Dr. Margaret McManus for continuous support, patience, motivation, and for her thoughtful academic and life advice; Gordon Walker for being my greatest role model, co-worker, and always encouraging me to think for myself; Chip Young and Dr. Chris Sabine for dedicating their time towards reviewing, and providing editing suggestions and encouragement on my report; Dr. James Potemra, Dr. Katharine Smith, and Christina Comfort for their amazing programming knowledge; the entire Pacific Islands Ocean Observing System family for treating me as one of their own; Dr. Barbara Bruno for her support; Han Quach for her love and kindness; Mom, Dad and Marisa; and my friends and the many students of the Global Environmental Science Program.

Abstract

Hawai‘i’s coastal ocean environments exhibit variability across a broad array of temporal and spatial scales, from short-term fluctuations like tidal forcing, heavy rain and wind events, to long-term fluctuations like El Niño-Southern Oscillation (ENSO), Pacific Decadal Oscillation (PDO), and global climate change. Such dynamic variability is difficult to scientifically describe, especially when environmental concerns including coastal water quality are of interest to the coastal community and ocean researchers. The Pacific Islands Ocean Observing System (PacIOOS) Nearshore Sensor Group monitors and measures coastal waters to determine the influences that water coming from both land and sea have on the nearshore environment. The installment of nearshore monitoring stations captures a wide spectrum of water quality parameters along the south shore of the island of O‘ahu, Hawai‘i. A twelve-year time-series of water quality data provided the foundation for quantifying water quality conditions across Mamala and Maunalua Bay and allowed for us to make connections between some of the environmental processes described here. Data from this collaboration shows increasing trends in water column temperature, chlorophyll *a*, turbidity, and pressure (depth); and decreasing trends in salinity. These data reveal a changing coastal environment, and the parameters stated above will affect O‘ahu’s coastal ecosystems and nearshore, urban setting. Hawai‘i is undergoing difficult decisions in planning to combat the effects of global climate change. Thus, the data provided in this collaboration can be a valuable contribution towards Hawai‘i’s climate change strategy and may benefit in the states approach to adaptation, resiliency, and future planning, to protect both the urban and coastal environments.

Contents

List of Tables

List of Figures

1.0 Introduction

The island of O‘ahu is the third largest island in the State of Hawai‘i, formed from the Wai‘anae and Ko‘olau shield volcanoes. The landscape of O‘ahu ranges from broad coastal plain to sheer interior mountain ranges (Oki and Brasher, 2003). The structure and form of these two ranges, along with erosional processes that have modified the original surfaces of the volcanoes, determine O‘ahu’s hydrologic setting (Oki and Brasher, 2003). Typical trade wind weather from the north east regularly brings diverse orographic rainfall to the central parts of the island. Heavy rain brings storm runoff down Hawai‘i’s steep watersheds, elevating stream flow, and bringing sediment and freshwater pulses to coastal environments, affecting nearshore water quality (De Carlo *et al.*, 2007). To quantify changes or emerging issues with coastal water quality, it is valuable to characterize waters by observing trends over both short and long-term time frames.

The Pacific Islands Ocean Observing System (PacIOOS) collects real-time data on ocean conditions, forecasts future events, and has developed user-friendly, publicly available tools to access information, which aims to promote safe, productive, and resilient coastal areas (https://www.pacioos.hawaii.edu/). Based within the School of Ocean and Earth Science and Technology (SOEST) at the University of Hawai‘i at Mānoa, PacIOOS addresses ocean observing needs on both a local and regional scale, working closely with a range of stakeholders throughout the U.S. Pacific Islands. The PacIOOS, O‘ahu Nearshore Senor Group manages nearshore sensor packages deployed throughout the Insular Pacific and Hawaiian Islands, including four long-term sensor packages along the south shore of O‘ahu. This group forms the base of this paper.

This collaborative effort focuses on water quality parameters gathered as long-term (~2008 - 2020) time-series data through maintaining monitoring stations along O‘ahu’s South Shore. High-resolution, four-minute interval data were measured over more than a decade to help us better understand coastal water quality and the spatial and temporal trends present in a changing environment and under a range of conditions (e.g., trade winds, relaxation of trade winds, tidal forcing’s, heavy rain events, global patterns, and climate change). Four *in situ* sensor packages are deployed at varying depths (0.5 – 2.0 m) in the nearshore ocean to collect long-term measurements of temperature, conductivity (salinity), pressure (depth), fluorescence (chlorophyll), and light attenuation (turbidity). Data from these four sensors are utilized to characterize variability in the water-column properties within Mamala and Maunalua Bay, O‘ahu. The analysis of these data supports the

ongoing work of PacIOOS and the Nearshore Sensor Group. The central goal of this research is to better understand water quality properties along O‘ahu’s South Shore, with efforts to establish connections between local trends and long-term environmental processes and patterns, including global climate change. Ultimately, encouraging action in the state’s efforts to adapt, plan, and implement policies to protect our coastal communities against the effects of climate change on oceans and sea levels.

2.0 Methods

2.1 Study Site

Our study site encompasses the coastal waters of the south shore of the island of Oʻahu, Hawaiʻi. Four PacIOOS Nearshore Sensors are deployed throughout Mamala and Maunalua Bay. The Nearshore Sensor packages are comprised of oceanographic sensors from Sea-Bird Electronics, specifics of which are discussed in Section 2.3. The Hawaiʻi Yacht Club sensor (NS02), the Atlantis Submarine Dock sensor (NS03), and the Waikiki Aquarium Sensor (NS04) are in Mamala Bay. The Maunalua Bay sensor (NS10) is located in Maunalua Bay (Figure 1). Site location was chosen based on highest human density, the amount of activity in each bay, and suitable deployment areas. The number and type of sensors utilized for sampling relates to funding for the project. Focus began in Waikiki on the Lē'ahi or Diamond Head side of the Ala Wai due to known plume movement. Deployment technique at each site varies. NS02 is attached to the end of a floating boat dock at the mouth of the Ala Wai Harbor. The sensor is positioned vertically in the water column 0.5 m below the surface, and free moving with tidal influence (Figure 2). NS03 is fixed to a mooring beneath the Atlantis Submarine dock, positioned vertically in the water column 1.0 m below the surface (Figure 3). NS04 is fixed on an inflow pipe outside of the Waikiki aquarium, positioned horizontally in the water column 2.0 m below the surface (Figure4). NS10 is fixed on a pylon in Maunalua Bay, just outside Koko Marina, positioned vertically in the water column 2.0 m below the surface (Figure 5).

Figure 1. Location of PacIOOS Nearshore Sensors along Oʻahu's South Shore (Google Earth Pro).

Figure 2: Placement of Nearshore Sensor at the Hawai‘i Yacht Club (NS02).

Figure 3: Placement of Nearshore sensor at the Atlantis Submarine Dock (NS03).

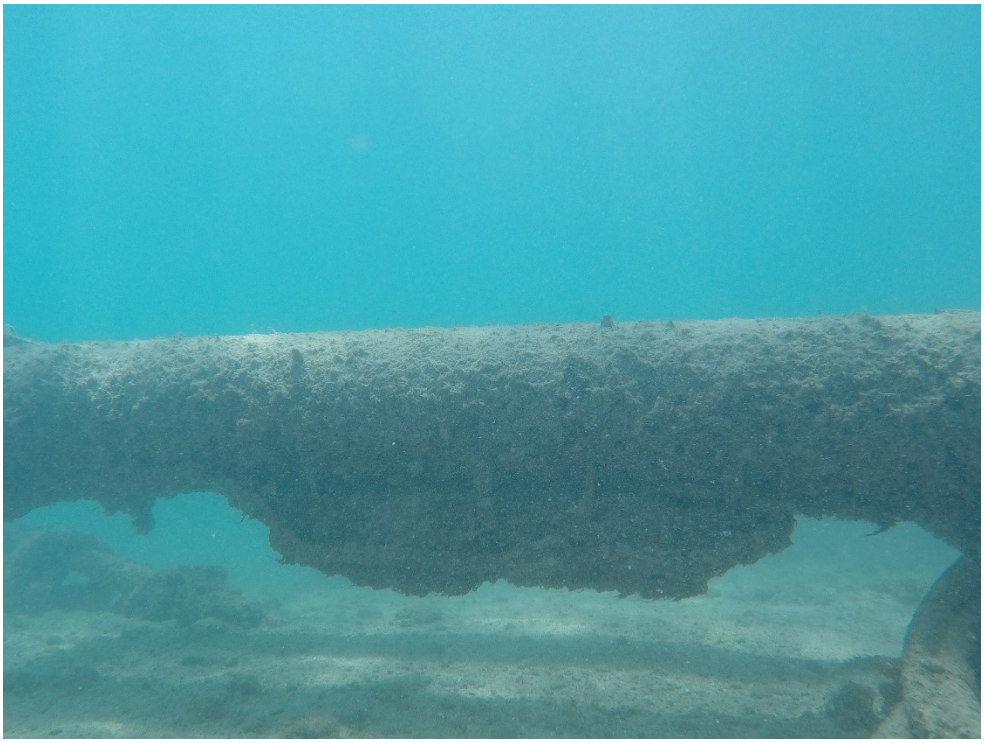

Figure 4: Placement of Nearshore Sensor at the Waikiki Aquarium (NS04).

Figure 5: Placement of Nearshore Sensor at Maunalua Bay (NS10).

2.2 Timeline of Deployment

PacIOOS Nearshore Sensors have been deployed over the past twelve years, from 2008 until present. NS02 was first deployed at the Hawai‘i Yacht Club boat dock, in July 2008, NS03 was first deployed at the Hilton Hawaiian Atlantis Submarine dock in January 2009, NS04 was first deployed outside the Waikiki Aquarium in September 2009, and NS10 was first deployed outside Koko Marina in Maunalua Bay in May 2011 (Figure 6). A large gap in data occurred for NS02 due to the 2011 Tōhoku earthquake and tsunami, which caused damages to the boat dock. Gaps in data for all other sites are largely due to the maintenance/servicing of sensors and sensor packages.

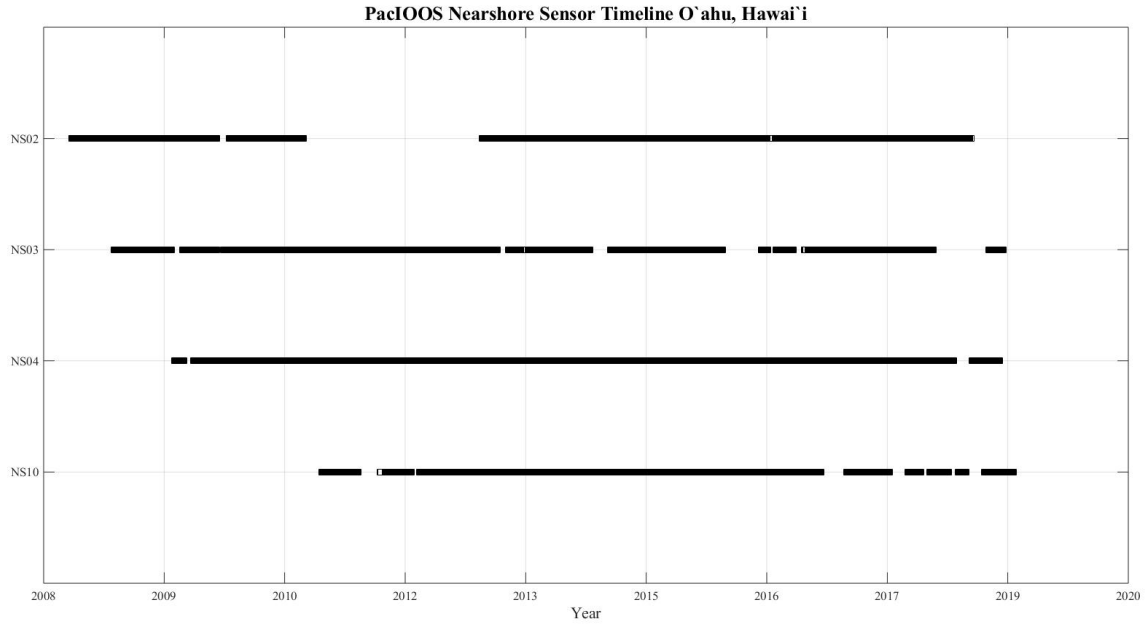

Figure 6. Time bar plot measured from 2008 – 2019 for the O‘ahu PacIOOS Nearshore Sensors. Gaps in data records indicate sensor issues, e.g., maintenance/servicing at manufacturer, or natural disturbances.

2.3 Sensors and Data Transmission

Sensor packages at NS02 and NS10 consist of Sea-Bird Electronics (SBE) 16plus V2 SeaCAT. Sensor packages at NS03 and NS04 consist of SBE 37 SMP MicroCAT. All packages record temperature and conductivity (salinity). NS03, NS04 and NS10 record pressure (depth): NS02 is attached to a floating dock, pressure is not measured. Sites that utilize the 16plus V2 SeaCAT RS-232’s are equipped with SBE WET Labs Environmental Characterization Optics (ECO) double-channel fluorometers for the measurement of relative fluorescence (chlorophyll) and light attenuation (turbidity). The ECO uses an LED to directly measure

the amount of fluorescence emission in a sample volume of water. Each sensor package is capable of autonomous recording up to three months after programming. Battery life and bio fouling limit the duration of deployment. We find that the sensors measure most accurately during cooler, winter months (November – April), and exhibit longer battery life (2 – 3 months). Summer months (May – October) exhibit increased biofouling from warmer water and enhanced light levels, hindering accuracy and limiting battery life of the sensors (1 – 2 months). Sensors and sensor packages were calibrated prior to initial deployment at each monitoring site and are sent back to SBE and WET Labs every 1.5 – 2 years for routine maintenance and calibration. If issues arise with a sensor, they are sent back earlier. Discrete sampling should be taken and analyzed for each allowable parameter every deployment term between calibrations with SBE to validate the autonomous measurements and verify any drift.

Each sensor takes samples and records data on four-minute intervals, with 10-sample averages. This sample frequency was chosen because it provides a comprehensive dataset when accounting for data storage and power limitations of the sensor packages. Every 20 minutes, recorded data are telemetered to a server on the University of Hawai‘i at Mānoa campus via a wireless modem. NS02 utilizes a Sierra Wireless Raven XT modem; and NS03, NS04 and NS10 utilize a Raven RV50 LTE Generic modem. Data from NS02, NS03 and NS10 are broadcasted by a Sprint network tower, while data from NS10 is broadcast through a Verizon network tower. Data are then stored in a robust real-time streaming engine (DataTurbine), which is used to store data internally and autonomously generate near real-time graphs on the PacIOOS Nearshore Sensor Observations webpage. Sensors brought back to the lab for maintenance have their data set downloaded and any short-term gaps that may have occurred during sampling periods caused by power outages or lapses in cell service are added to the DataTurbine.

2.4 Data Analysis

For the analysis included herein, raw time-series data were gathered from both the sensors (during my time as a student), and from the publicly accessible, historic data collection on the PacIOOS Environmental Research Division’s Data Access Program (ERDDAP). All data processing, analysis, and visualization was completed within MATLAB R2018b. In order to understand trends in water quality on both temporal and spatial scales, MATLAB was used to generate a series of graphs comparing temperature, salinity, pressure,

chlorophyll and turbidity; as well as wind, rainfall, and global patterns like El Niño-Southern Oscillation (ENSO) and Pacific Decadal Oscillation (PDO). Data processing and trend review was conducted from Spring 2019 – Spring 2020. Sensor datasets were plotted as individual points, and trends were made using the polynomial curve fitting function (polyfit). Change over time for each parameter was determined from the slope of the fitted trend lines. Statistical analysis was completed using the correlations coefficient function (corrcoef). Daily – monthly moving averages were utilized to smooth datasets with the moving average function (movmean). Wind plots were made using the quiver and histogram functions. All other figures were made using basic plot functions within MATLAB.

3.0 Results

3.1 Temperature

Temperature measurements from each nearshore sensor show strong annual, seasonal and daily variability. Seasonally, ocean temperatures appear coolest in February (24.7 ºC) and warmest in September (27.6 ºC), averaged across all locations. In general, the Hawai‘i Yacht Club (NS02) displays a great amount of daily temperature fluctuation, and the second highest total range of high-frequency seasonal data from 22.0 – 31.9 ºC (Figure 7). Maunalua Bay (NS10) shows the greatest seasonal range of high-frequency data from 20.8 – 32.1 ºC (Figure 8), while the Atlantis Submarine Dock (NS03) (Figure 9) and The Waikiki Aquarium (NS04) (Figure 10) sensors fall in between (Table 1).

The average daily temperature at each site varies. NS02 presents the highest average daily temperature (26.8 ºC), consistently warmer than the other sites. NS04 has an average daily temperature of 25.9 ºC, and NS03 has an average daily temperature of 25.6 ºC. NS10 is consistently cooler, with an average daily temperature of 25.5 ºC. All four nearshore sites reveal a rise in near-surface temperature from the time of initial instillation until present (Table 1).

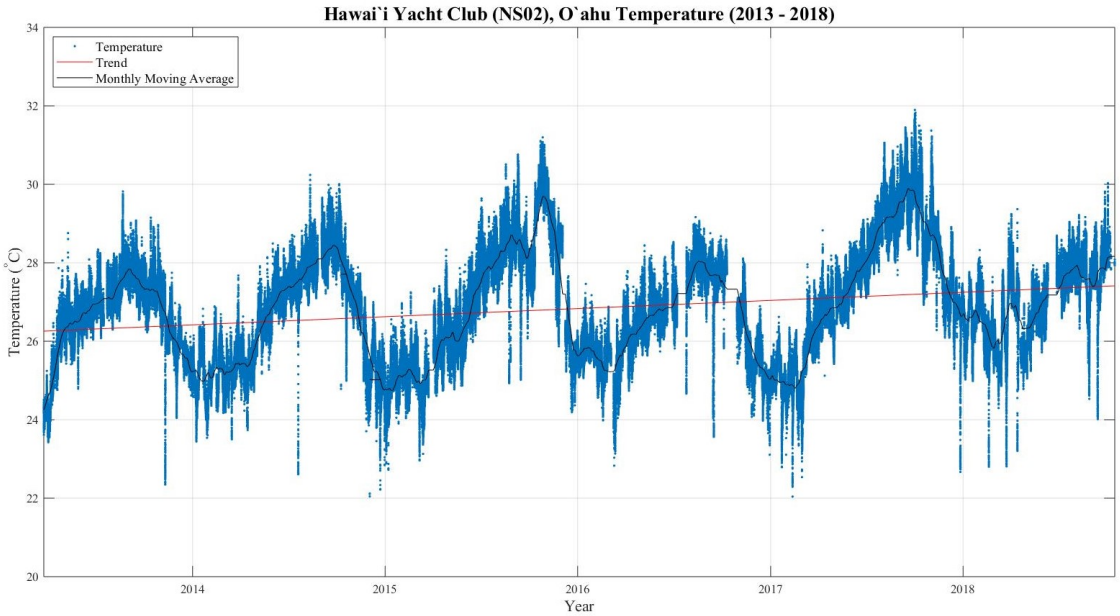

Figure 7. Temperature (ºC) measured from March 2013 – October 2018 in four-minute intervals at the Hawai‘i Yacht Club (NS02) Nearshore Sensor. Blue dots: temperature (ºC) measurement, black line: a monthly moving average, red line: fit line using polyfit function in MATLAB showing a 1.14 ºC trend in temperature over time.

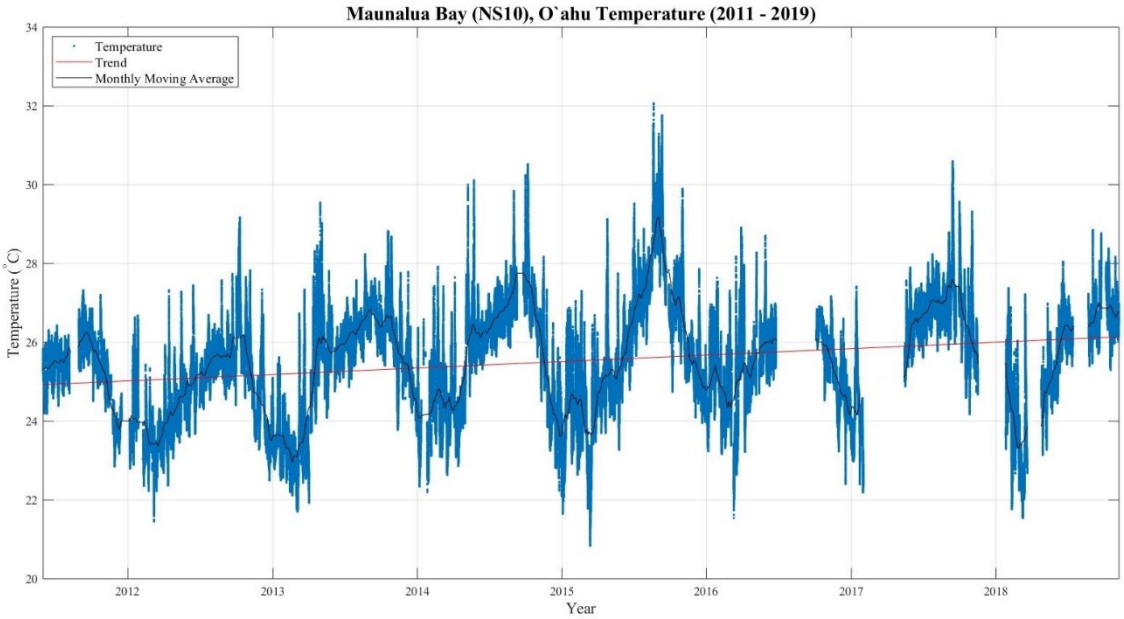

Figure 8. Temperature (ºC) measured from May 2011 – November 2018 in four-minute intervals for the Maunalua Bay (NS10) Nearshore Sensor. Blue dots: temperature (ºC) measurement, black line: a monthly moving average, red line: fit line using polyfit function in MATLAB showing a 1.21 ºC trend in temperature over time.

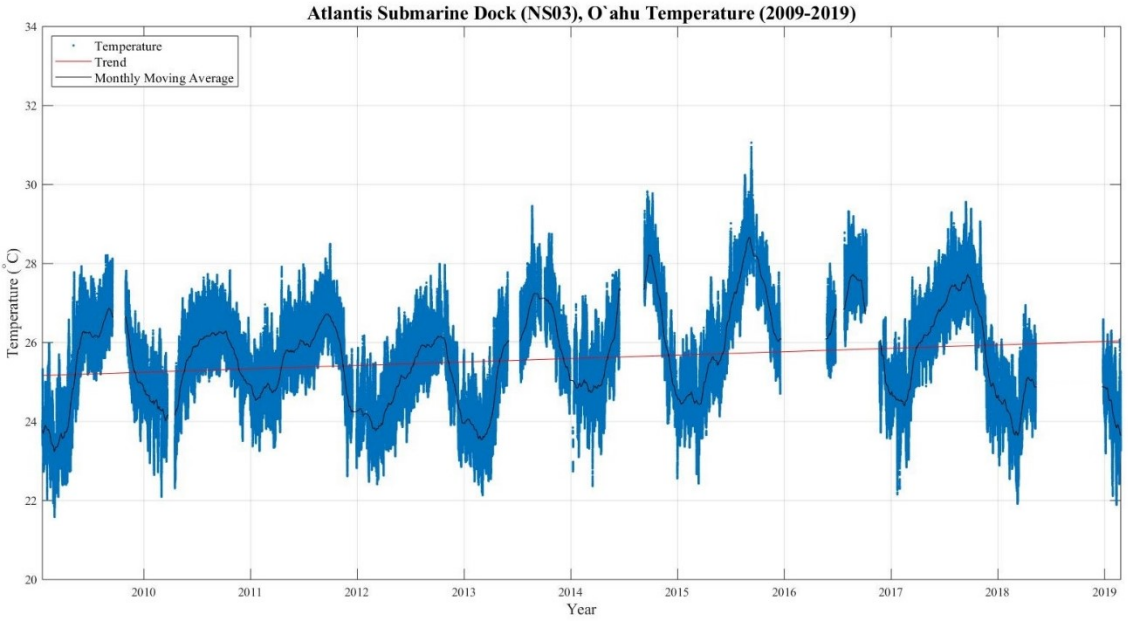

Figure 9. Temperature (ºC) measured from January 2009 – February 2019 in four-minute intervals for the Atlantis Submarine Dock (NS03) Nearshore Sensor. Blue dots: temperature(ºC) measurement, black line: a monthly moving average, red line: fit line using polyfit function in MATLAB showing a 0.87 ºC trend in temperature over time.

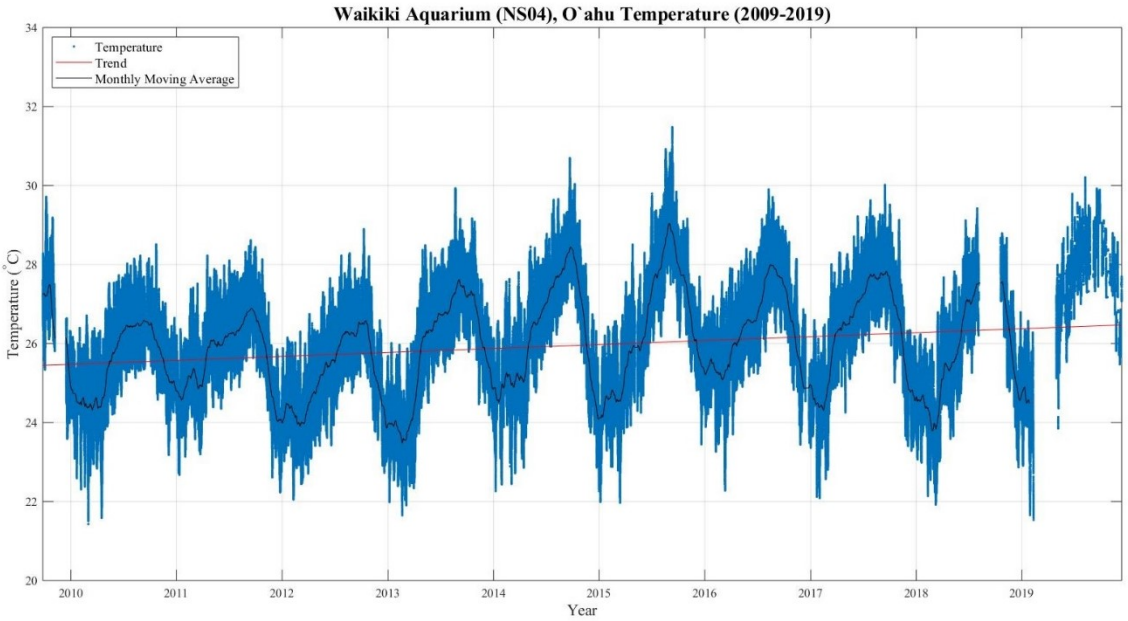

Figure 10. Temperature (ºC) measured from September 2009 – December 2019 in four-minute intervals at the Waikiki Aquarium (NS04) Nearshore Sensor. Blue dots: temperature (ºC) measurement, black line: a monthly moving average, red line: fit line using polyfit function in MATLAB showing a 1.02 ºC trend in temperature over time.

Nearshore Sensor	Highest Daily Temperature ºC	Lowest Daily Temperature ºC	Average Temperature ºC	Standard Deviation ± ºC	Change Over Time ºC	P-Value	R^2
NS02	31.90	22.00	26.80	1.40	1.14	< 0.01	0.06
NS03	31.10	21.60	25.60	1.30	0.87	< 0.01	0.03
NS04	31.50	21.40	25.90	1.40	1.02	< 0.01	0.04
NS10	32.10	20.80	25.50	1.40	1.21	< 0.01	0.06

Table 1. Varying aspects of temperature (ºC) for each nearshore sensor site across O‘ahu, including highest daily temperature, lowest daily temperature, average temperature, standard deviation, change in temperature over time, and statistical values.

3.2 Salinity

Salinity measurements vary across all four nearshore sensors. Unlike temperature, salinity for all four sites do not show strong seasonal or interannual variability. NS02 displays the greatest amount of fluctuation ranging from 1.7 practical salinity units (PSU) – 35.4 PSU, with an average of 33 PSU (Figure 11). NS10 displays the least amount of variability with the exception of a rain event on March 6th of 2012 ranging from 12.3 – 35.7 PSU, with an average of 35 PSU (Figure 12). NS03 fluctuates between 28.2 – 35.5 PSU, with an average of 34.9 PSU (Figure 13). NS04 displays fluctuations between 28.3 – 36.0 PSU, with an average of 34.9 PSU (Figure 14). All four nearshore sites portray a decline in overall salinity levels from initial installation until present (Table 2).

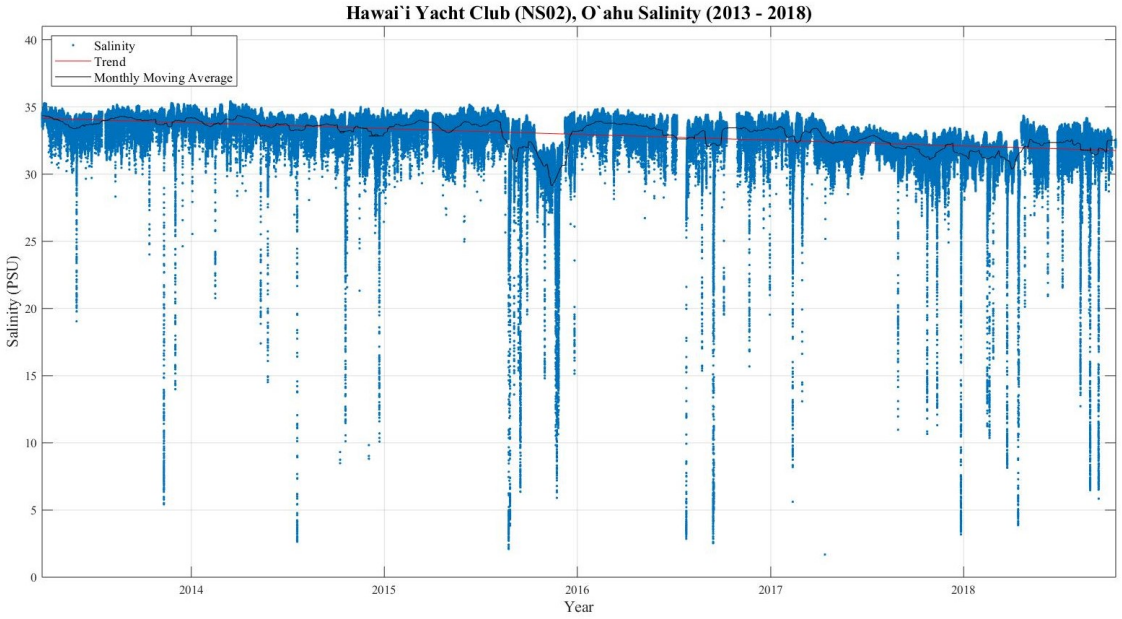

Figure 11. Salinity (PSU) measured from March 2013 – October 2018 in four-minute intervals at the Hawai‘i Yacht Club (NS02) Nearshore Sensor. Blue dots: salinity (PSU) measurement, black line: a monthly moving average, red line: fit line using polyfit function in MATLAB showing a -2.37 PSU trend in salinity over time.

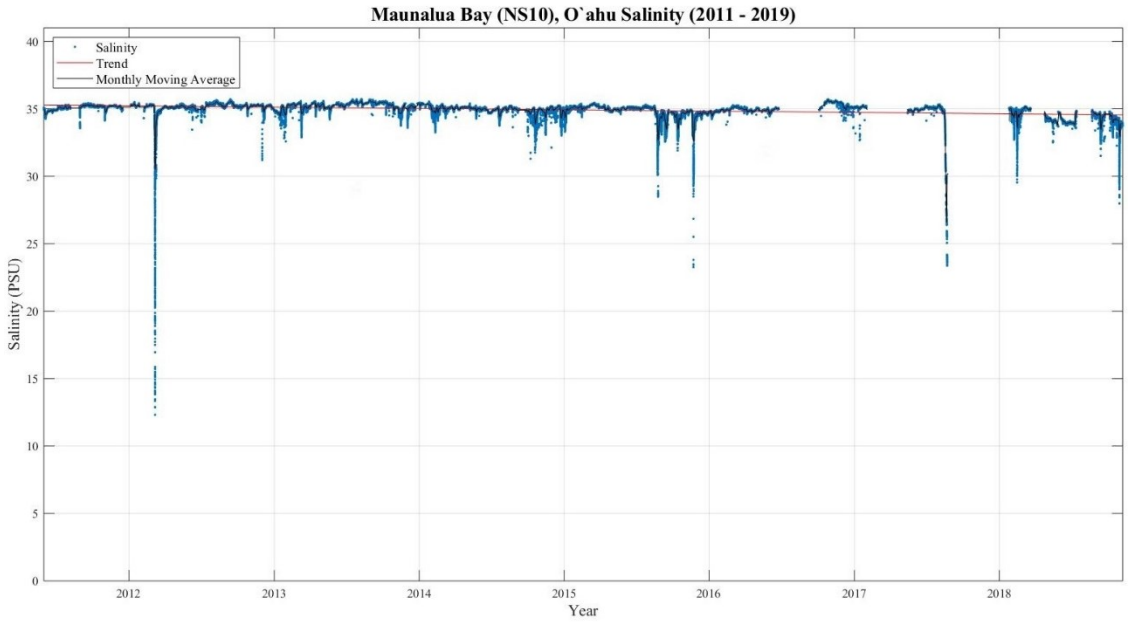

Figure 12. Salinity (PSU) measured from May 2011 – November 2018 in four-minute intervals for the Maunalua Bay (NS10) Nearshore Sensor. Blue dots: salinity (PSU) measurement, black line: a monthly moving average, red line: fit line using polyfit function in MATLAB showing a -0.73 PSU trend in salinity over time.

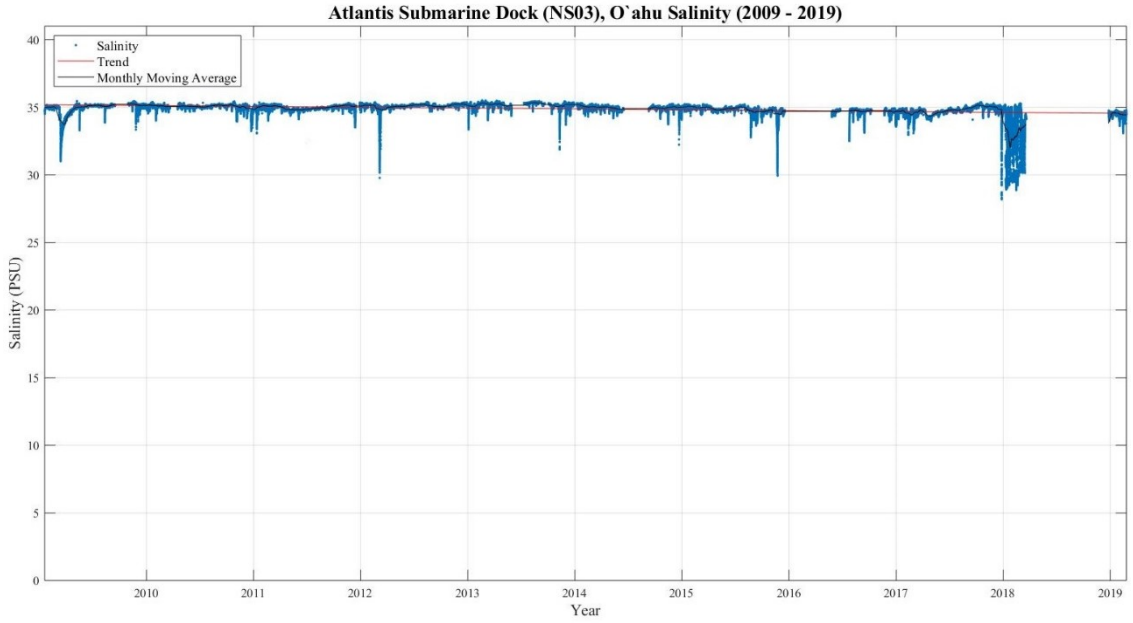

Figure 13. Salinity (PSU) measured from January 2009 – February 2019 in four-minute intervals for the Atlantis Submarine Dock (NS03) Nearshore Sensor. Blue dots: salinity (PSU) measurement, black line: a monthly moving average, red line: fit line using polyfit function in MATLAB showing a -0.64 PSU trend in salinity over time.

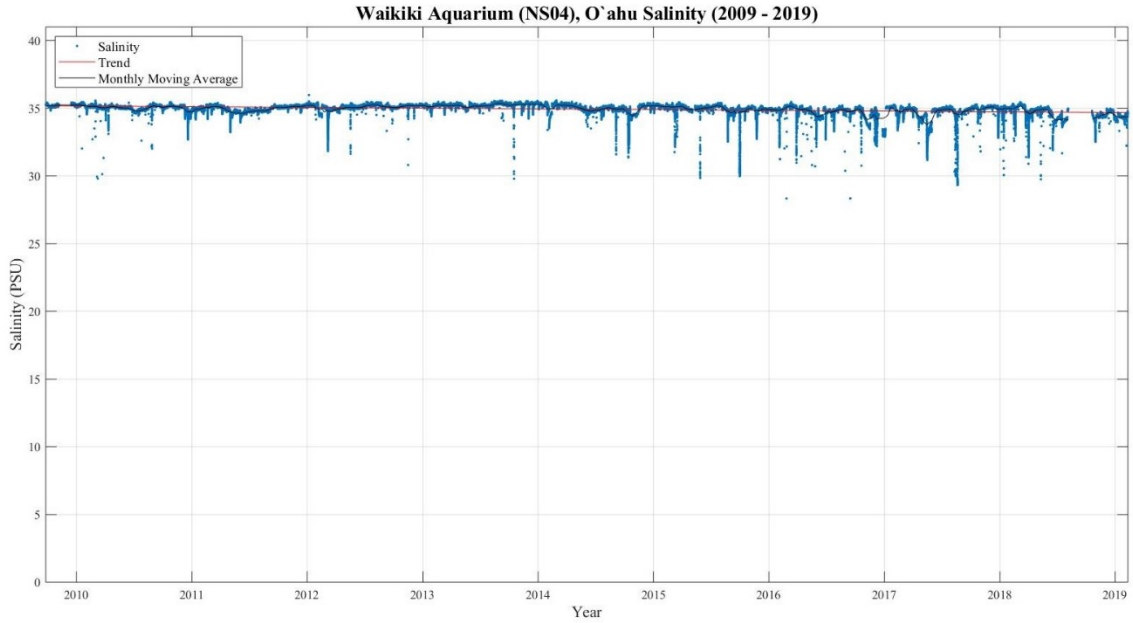

Figure 14. Salinity (PSU) measured from September 2009 – December 2019 in four-minute intervals at the Waikiki Aquarium (NS04) Nearshore Sensor. Blue dots: salinity (PSU) measurement, black line: a monthly moving average, red line: fit line using polyfit function in MATLAB showing a -0.54 PSU trend in salinity over time.

Nearshore Sensor	Highest Daily Salinity (PSU)	Lowest Daily Salinity (PSU)	Average Salinity (PSU)	Standard Deviation ± (PSU)	Change Over Time (PSU)	P-Value	R^2
NS02	35.40	1.70	33.00	2.00	-2.37	< 0.01	0.12
NS03	35.50	28.20	34.00	0.60	-0.64	< 0.01	0.10
NS04	35.90	28.30	35.00	0.40	-0.54	< 0.01	0.14
NS10	35.70	12.30	34.90	0.60	-0.73	< 0.01	0.12

Table 2. Varying aspects of salinity (PSU) for each nearshore sensor site across O‘ahu, including highest daily salinity, lowest daily salinity, average salinity, standard deviation, change in salinity over time, and statistical values.

3.3 Chlorophyll

Chlorophyll *a* measurements were taken for two nearshore sites (NS02 and NS10), however, only night-time chlorophyll *a* measurements are portrayed. Night-time chlorophyll *a* was analyzed to account for excess light during the day and nonphotochemical quenching, described further in Section 4.3. Samples were analyzed from 18:00:00 – 06:00:00 under our standard four-minute interval. This parameter, indicative of phytoplankton biomass, appeared more variable in NS02 (Figure 15), in comparison to NS10 (Figure 16). On average, NS02 measured 2.8 µg/L, whereas NS10 measured 1.1 µg/L. Both sensors show an increase in chlorophyll *a* concentrations from the time of site instillation to present day (Table 3).

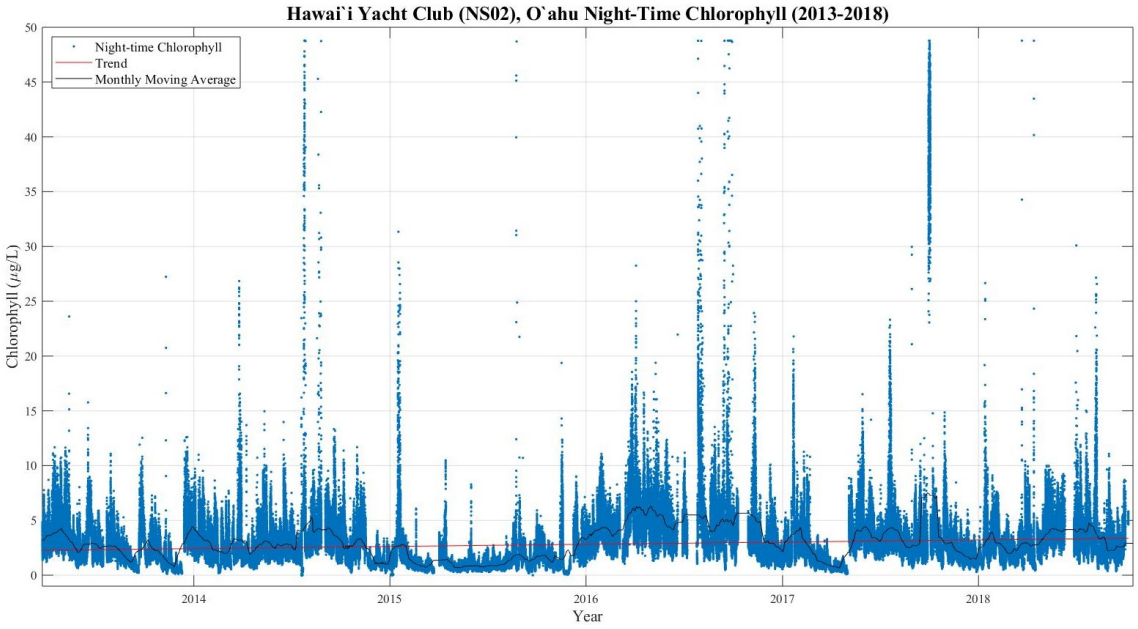

Figure 15. Chlorophyll (µg/L) measured from March 2013 – October (2018) in four-minute intervals at the Hawai‘i Yacht Club (NS02) Nearshore Sensor. Blue dots: Chlorophyll (µg/L) measurement, black line: a monthly moving average, red line: fit line using polyfit in MATLAB showing a 1.09 µg/L trend in chlorophyll over time.

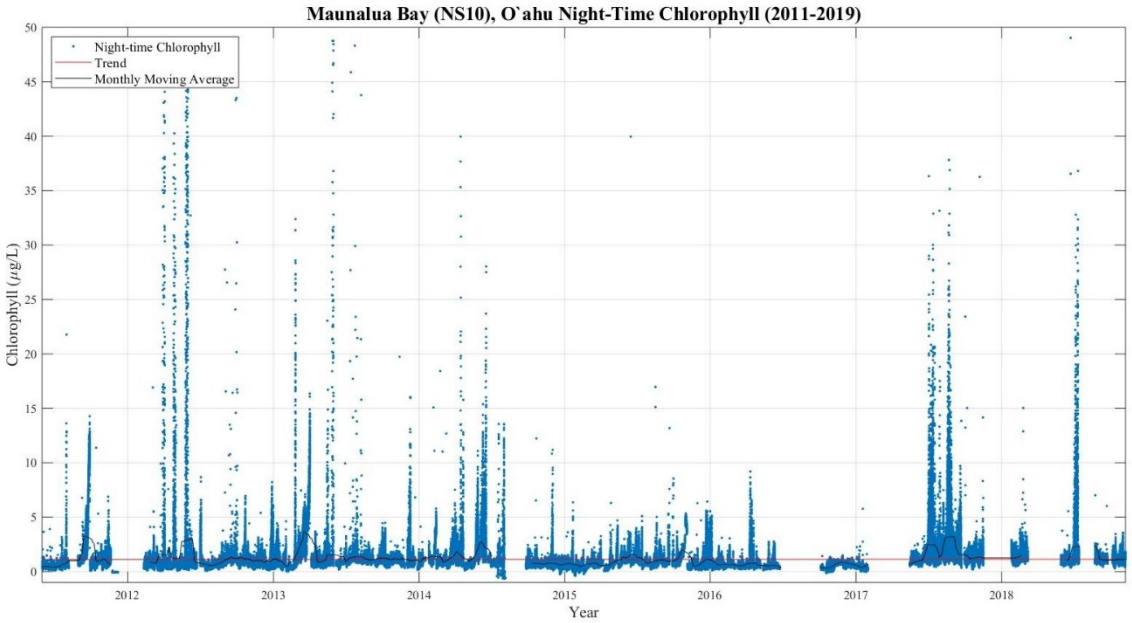

Figure 16. Chlorophyll (µg/L) measured from May 2011 – November 2018 in four-minute intervals for the Maunalua Bay (NS10) Nearshore Sensor. Blue dots: chlorophyll (µg/L) measurement, black line: a monthly moving average, red line: fit line using polyfit function in MATLAB showing a 0.03 µg/L trend in chlorophyll over time.

Nearshore Sensor	Highest Daily Chlorophyll (µg/L)	Lowest Daily Chlorophyll (µg/L)	Average Chlorophyll (µg/L)	Standard Deviation ± (µg/L)	Change Over Time (µg/L)	P-Value	R^2
NS02	49.80	-0.04	2.80	3.10	1.09	< 0.01	0.01
NS10	49.00	-0.64	1.10	2.10	0.03	< 0.01	0.00

Table 3. Varying aspects of chlorophyll (µg/L) for both NS02 and NS10, including highest daily chlorophyll level, lowest daily chlorophyll level, average chlorophyll, standard deviation, change in chlorophyll over time, and statistical values.

3.4 Turbidity

Turbidity measurements were taken for two nearshore sensor sites (NS02 and NS10). However, these two sites are not on similar ranges due to manufacturer calibration settings of the ECO fluorometer. NS02 has a max range of 100 NTU, whereas NS10 has a max range of 25 NTU. These varying coefficients give both sensors different maximum measured turbidity values, placing NS10's highest NTU measurement far below NS02. Overall comparisons between each site were not completed because of this, and NS10 is not shown in the results section. NS02 displays an average of 2.1 NTU over the course of installation until present time (Figure 17), and an overall increase in turbidity over time (Table 4).

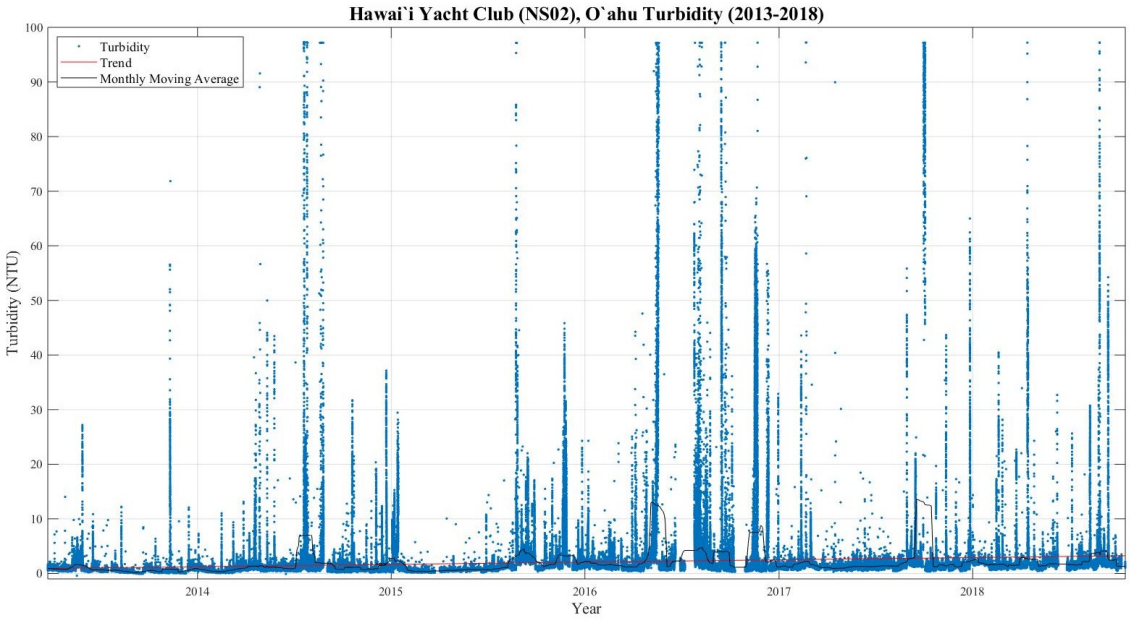

Figure 17. Turbidity (NTU) measured from March 2013 – October 2018 in four-minute intervals at the Hawai'i Yacht Club (NS02) Nearshore Sensor. Blue dots: turbidity (NTU) measurement, black line: a monthly moving average, red line: fit line using polyfit function in MATLAB showing a 2.31 NTU trend in turbidity over time.

Nearshore Sensor	Highest Daily Turbidity (NTU)	Lowest Daily Turbidity (NTU)	Average Turbidity (NTU)	Standard Deviation ± (NTU)	Change Over Time (NTU)	P-Value	R^2
NS02	97.20	-0.42	2.06	7.10	2.31	< 0.01	0.01

Table 4. Varying aspects of Turbidity (NTU) for NS02, including highest daily turbidity level, lowest daily turbidity level, average turbidity, standard deviation, change in turbidity over time, and statistical values.

3.5 Pressure

Three of the four sensor locations have pressure data; however, pressure was only analyzed at one nearshore sensor site (NS04). This location offers the only fixed mooring that allows for horizontal placement of the CTD, required for measuring pressure. This fixed placement admits for precise re-deployment at a specific depth for more accurate pressure measurements. NS04 exhibits an average depth of 1.9 m, and a slope of 0.03 m, over the course of installation until present day (Figure 18).

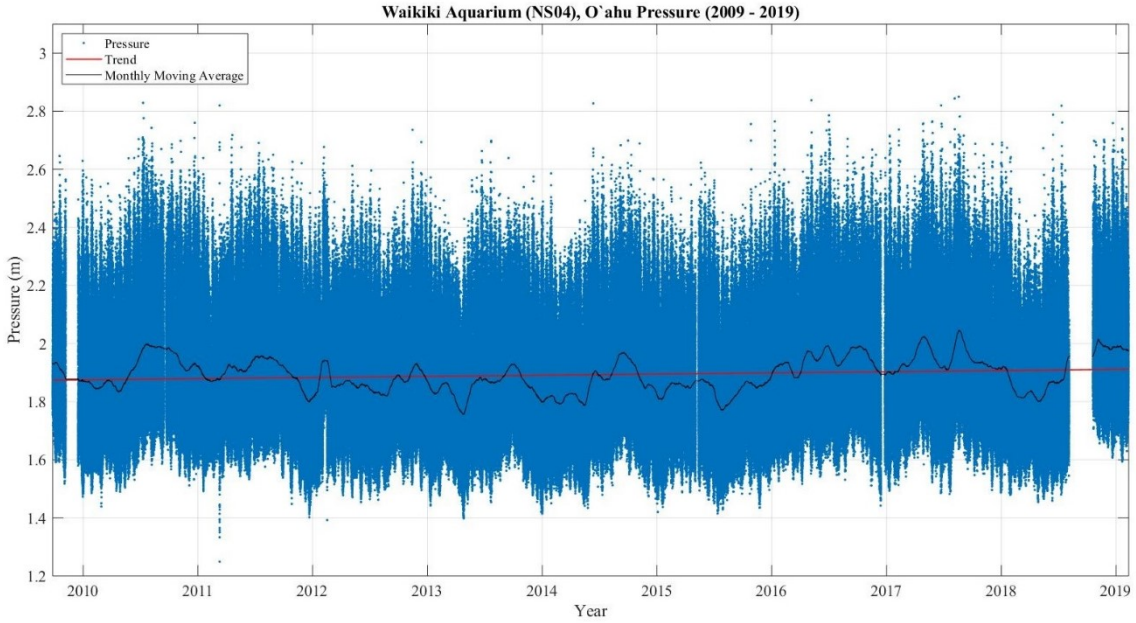

Figure 18. Pressure (m) measured from September 2009 – December 2019 in four-minute intervals at the Waikiki Aquarium (NS04) Nearshore Sensors. Blue dots: pressure (m) measurement, black line: a monthly moving average, red line: fit line using polyfit function in MATLAB showing a 0.03 m trend in pressure over time.

Nearshore Sensor	Highest Daily Pressure (m)	Lowest Daily Pressure (m)	Average Pressure (m)	Standard Deviation ± (m)	Change Over Time (m)	P-Value	R^2
NS04	2.90	1.20	1.90	0.19	0.03	< 0.01	0.00

Table 5. Varying aspects of Pressure (m) for NS04, including highest daily pressure level, lowest daily pressure level, average pressure, standard deviation, change in pressure over time, and statistical values.

3.6 Rainfall

Rain data was taken from the United States Geological Survey (USGS) Moanalua rain gauge from 2007 – 2019. This record showed seasonal and inter-annual patterns (Figure 19). Long-term data shows neither an increase nor decrease in rainfall over the course of this study.

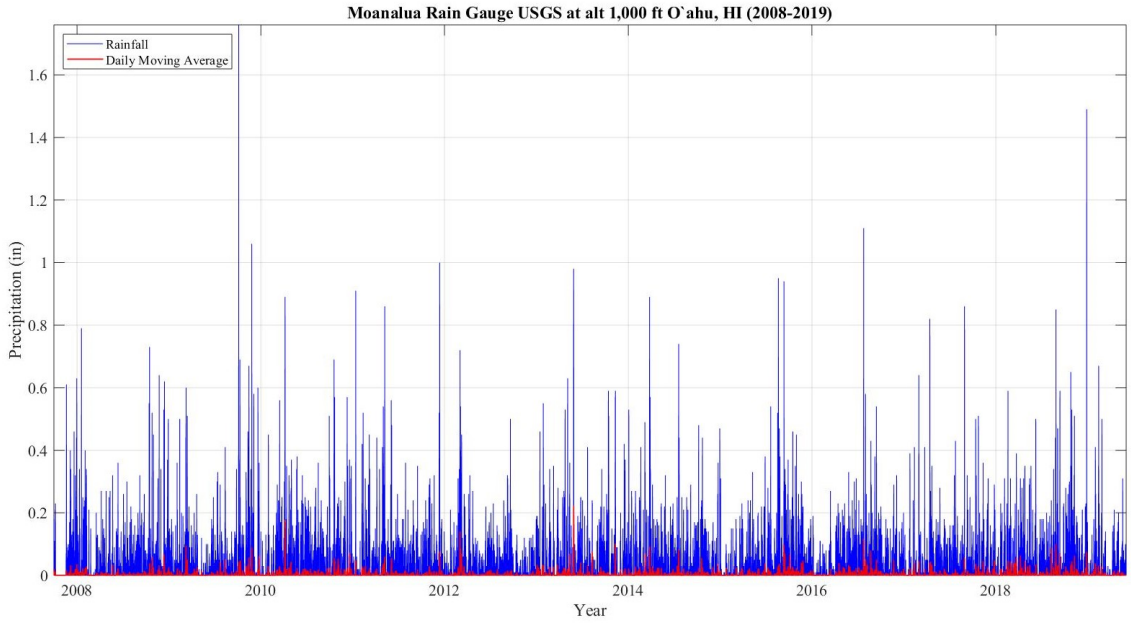

Figure 19. Fifteen minute rainfall data (in) from Moanalua, O‘ahu at an elevation of 1,000 ft from 2008 – 2019. Blue represents rainfall data. Red represents a daily moving average.

3.7 Wind

Tracking changes in Hawai‘i’s wind patterns over the course of this collaboration is important to understand the frequency and intensity of the shifts between prevailing trade winds and southern Kona winds. Wind data was taken from the National Weather Service Honolulu International Airport wind station from 2000 – 2020. This record for the region shows changes in directional frequency over time (Figure 20). Over the course of study, trade winds remain the dominant pattern (n = 4404), compared to southern or Kona winds (n = 2939) (Figure 21 - 22). The frequency of trade winds has decreased over time, while the frequency of Kona winds has increased (Figure 23 - 43).

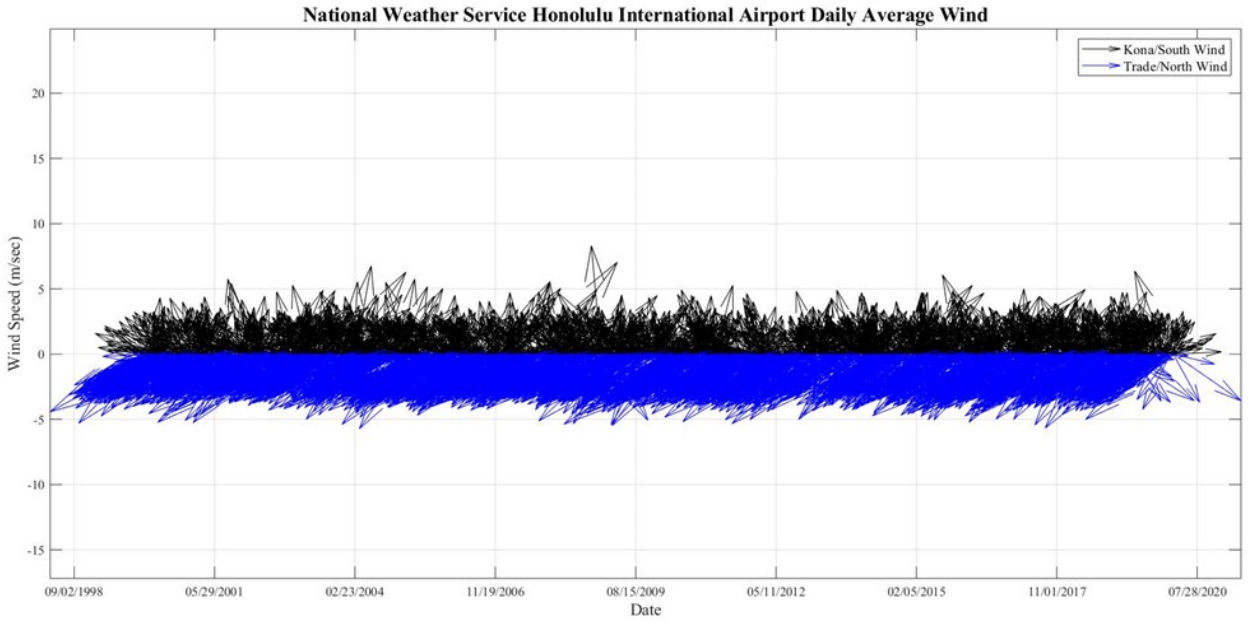

Figure 20. Daily average winds from the National Weather Service at the Honolulu International Airport from 2000 – 2020. Black vectors represent speed and direction of Kona wind/southern winds. Bluc vectors represent speed and direction of tradewind/north winds.

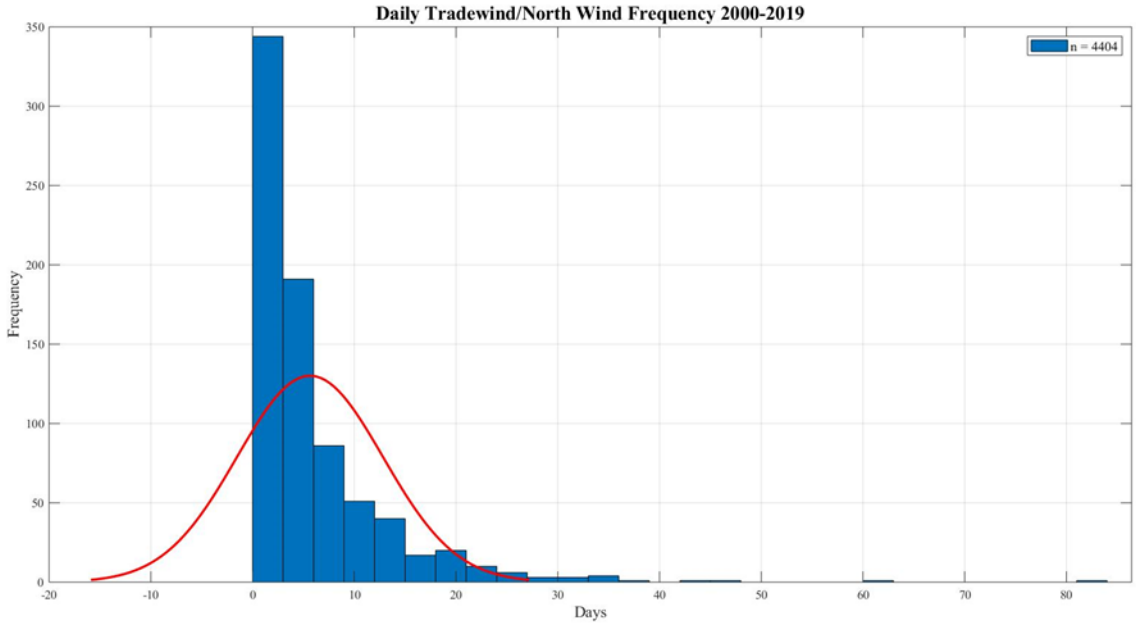

Figure 21. Daily tradewind/north wind frequencies at the National Weather Service at the Honolulu International Airport from 2000 – 2020. Blue bars represents the frequency of tradewind/north wind, n = 4404. Red line represents a histogram fit line.

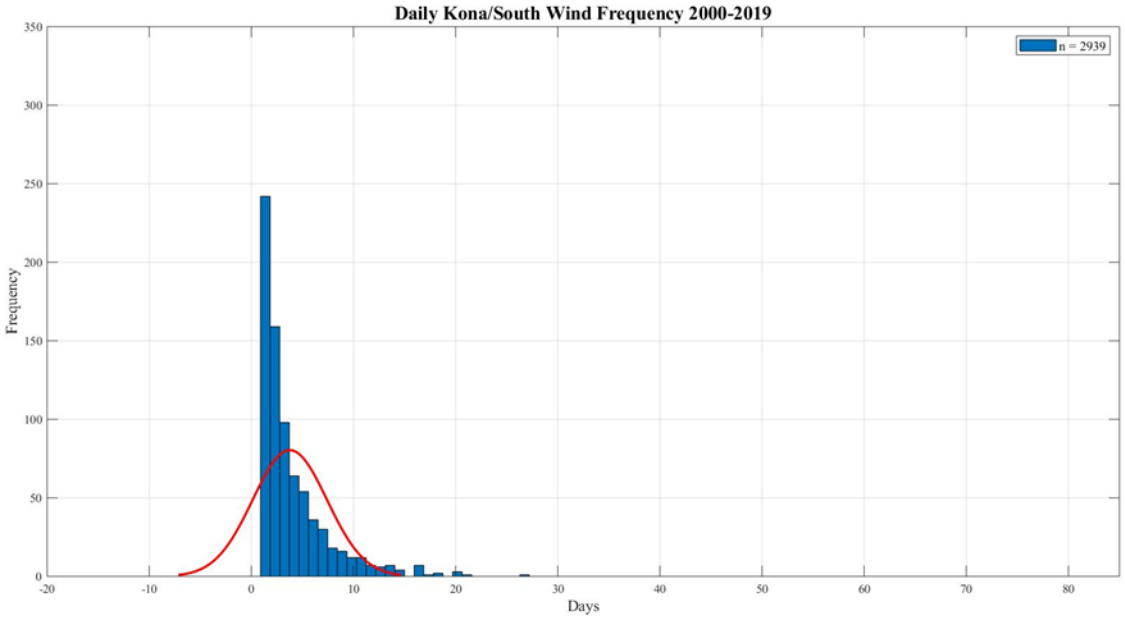

Figure 22. Daily Kona wind/south wind frequencies at the National Weather Service at the Honolulu International Airport from 2000 – 2020. Blue bars represents the frequency of Kona wind/south wind, n = 2939. Red line represents a histogram fit line.

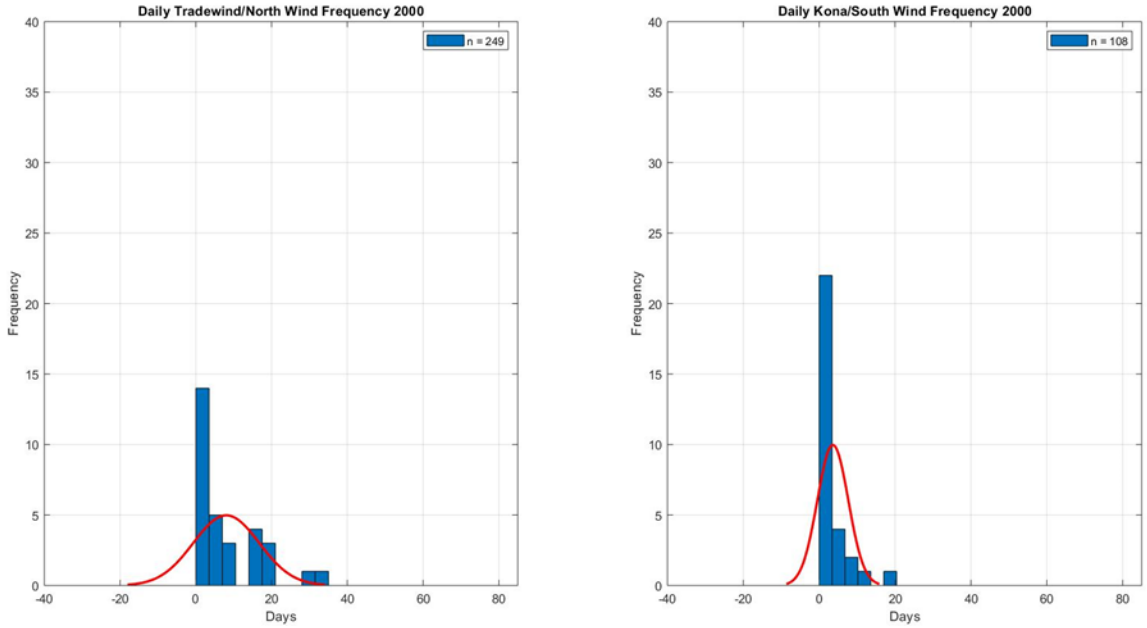

Figure 23. Daily Tradewind/north wind vs. Kona/south wind frequencies for year 2000 at the National Weather Service at the Honolulu International Airport.

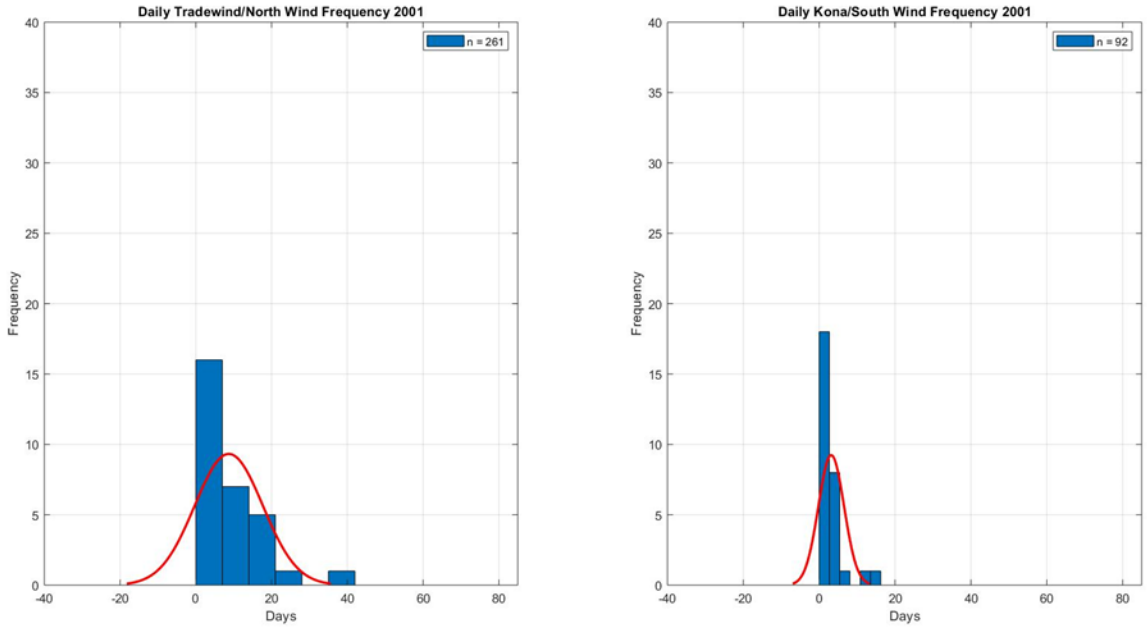

Figure 24. Daily Tradewind/north wind vs. Kona/south wind frequencies for year 2001 at the National Weather Service at the Honolulu International Airport.

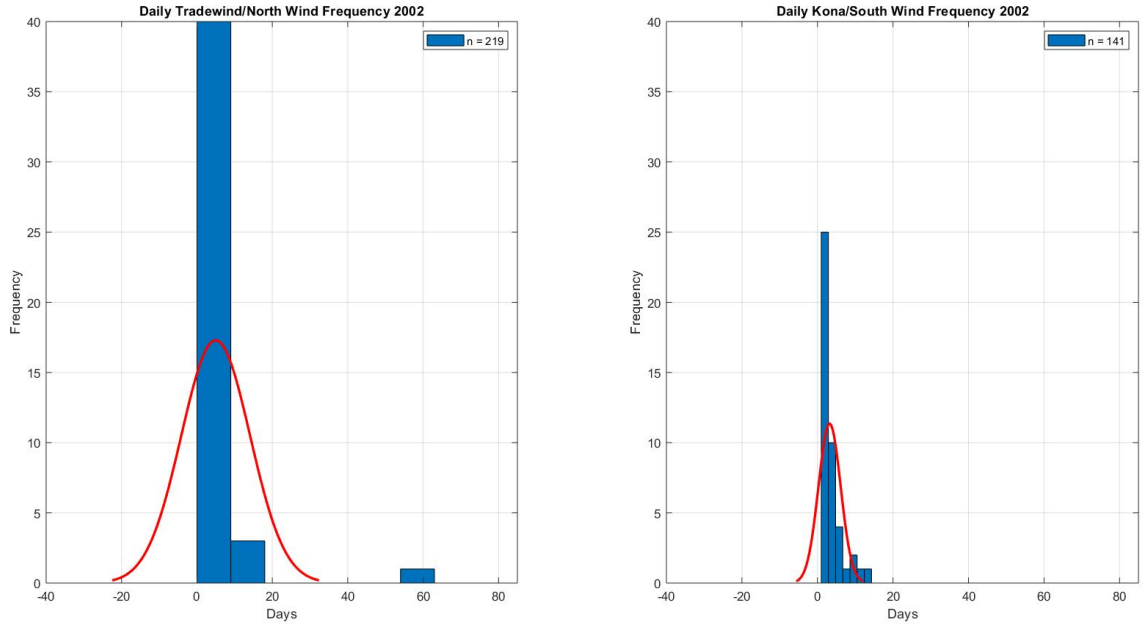

Figure 25. Daily Tradewind/north wind vs. Kona/south wind frequencies for year 2002 at the National Weather Service at the Honolulu International Airport.

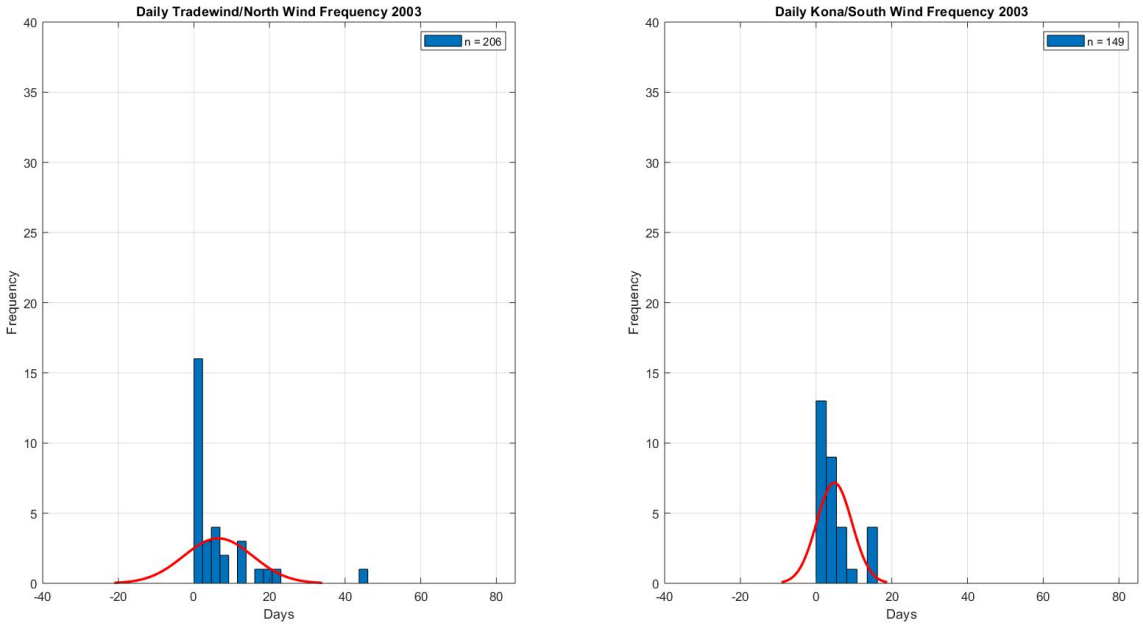

Figure 26. Daily Tradewind/north wind vs. Kona/south wind frequencies for year 2003 at the National Weather Service at the Honolulu International Airport.

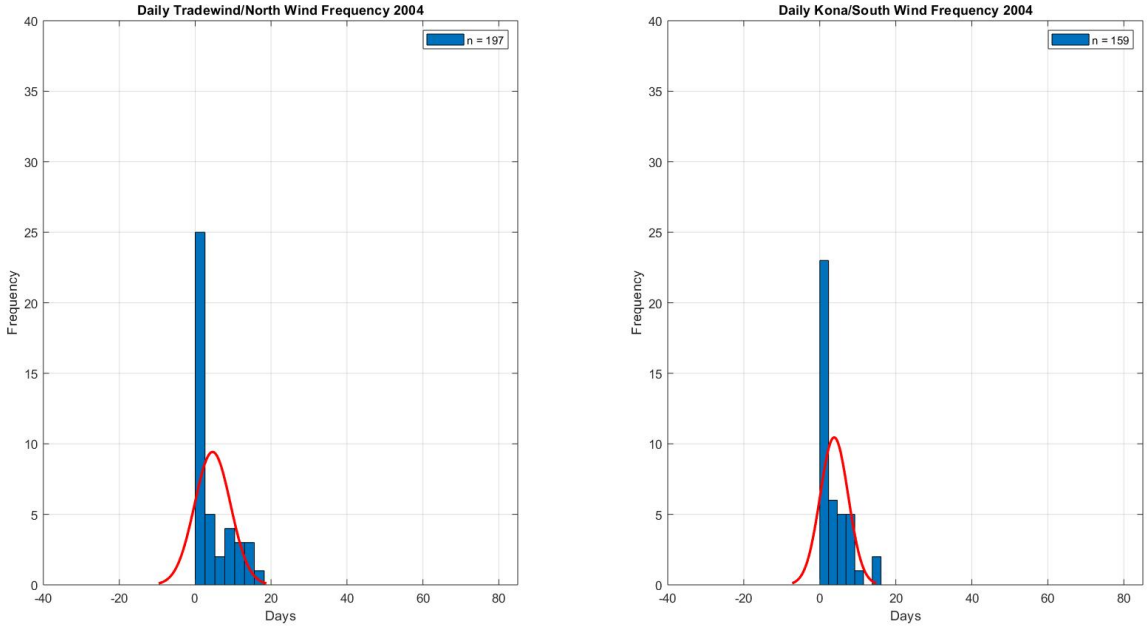

Figure 27. Daily Tradewind/north wind vs. Kona/south wind frequencies for year 2004 at the National Weather Service at the Honolulu International Airport.

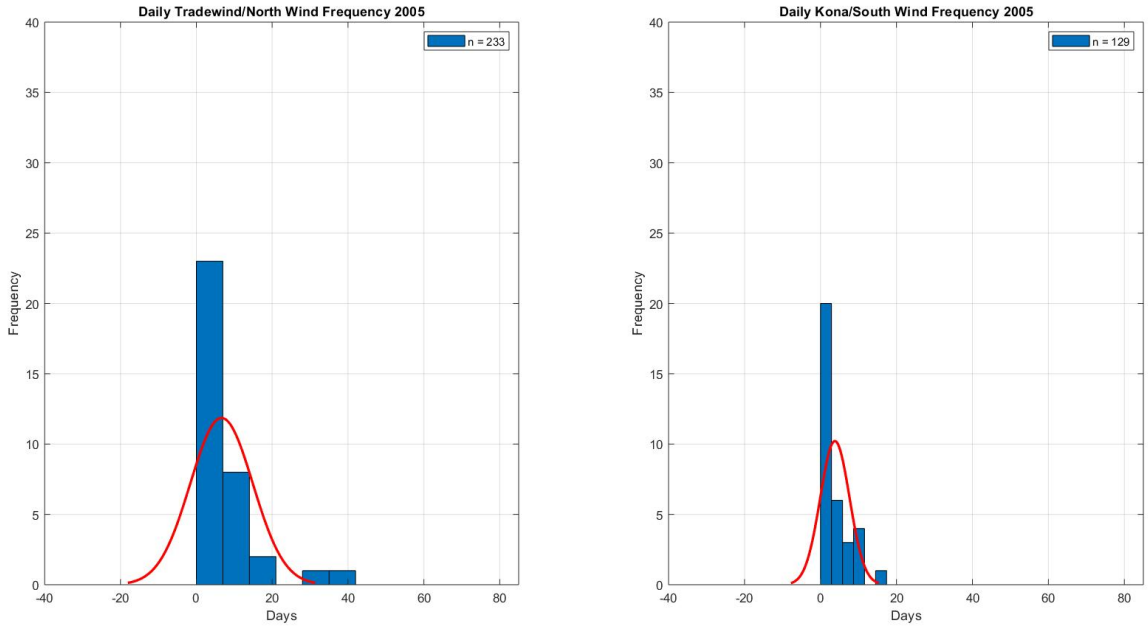

Figure 28. Daily Tradewind/north wind vs. Kona/south wind frequencies for year 2005 at the National Weather Service at the Honolulu International Airport.

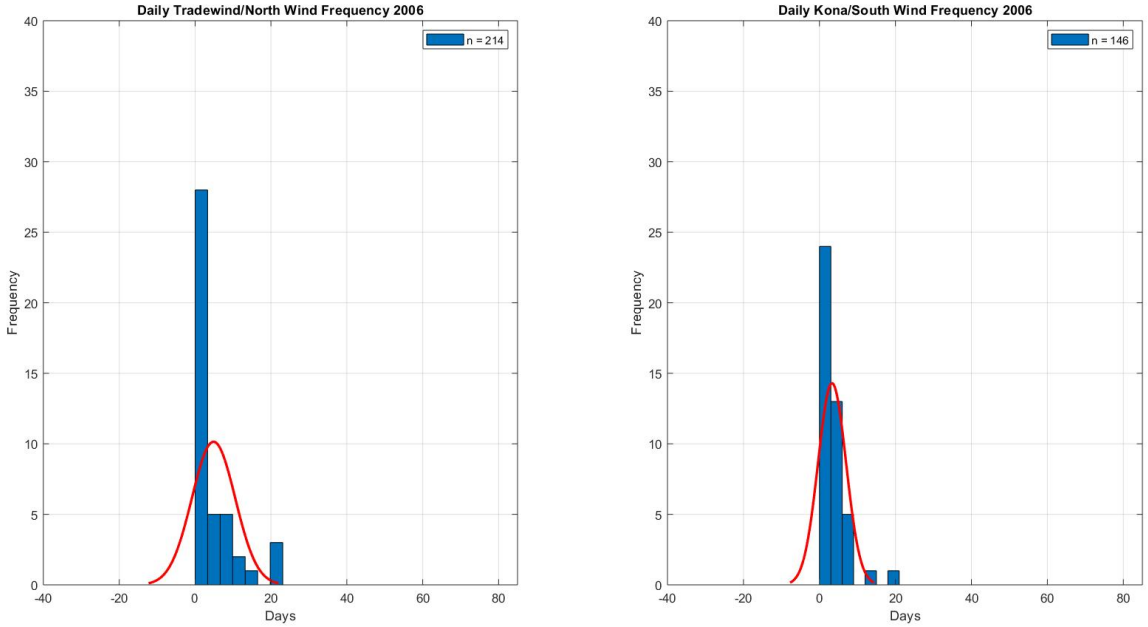

Figure 29. Daily Tradewind/north wind vs. Kona/south wind frequencies for year 2006 at the National Weather Service at the Honolulu International Airport.

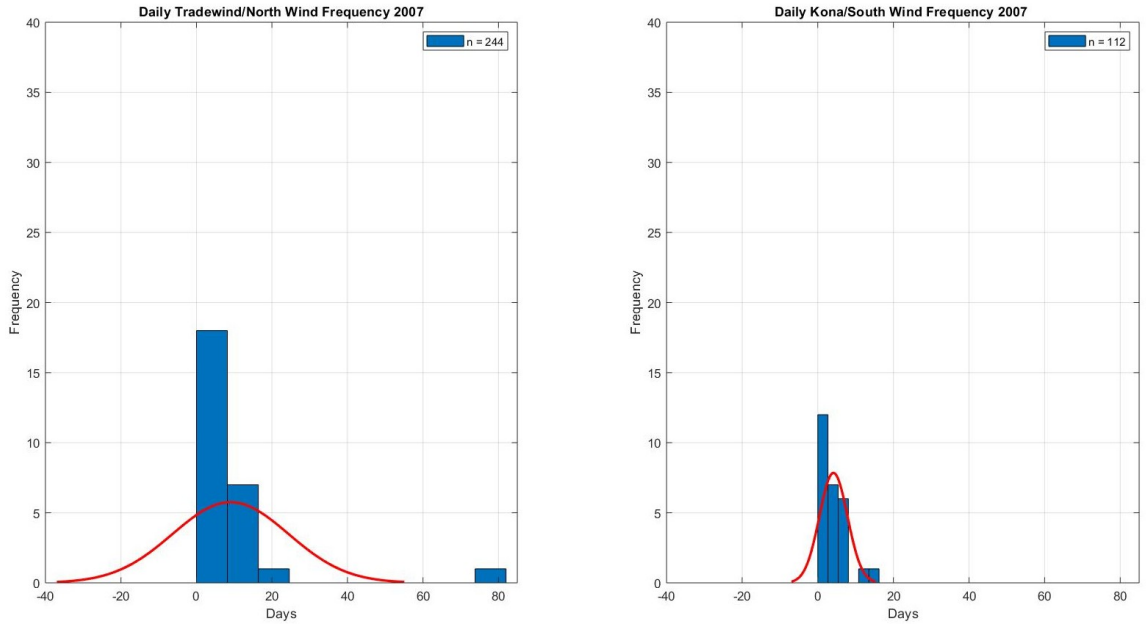

Figure 30. Daily Tradewind/north wind vs. Kona/south wind frequencies for year 2007 at the National Weather Service at the Honolulu International Airport.

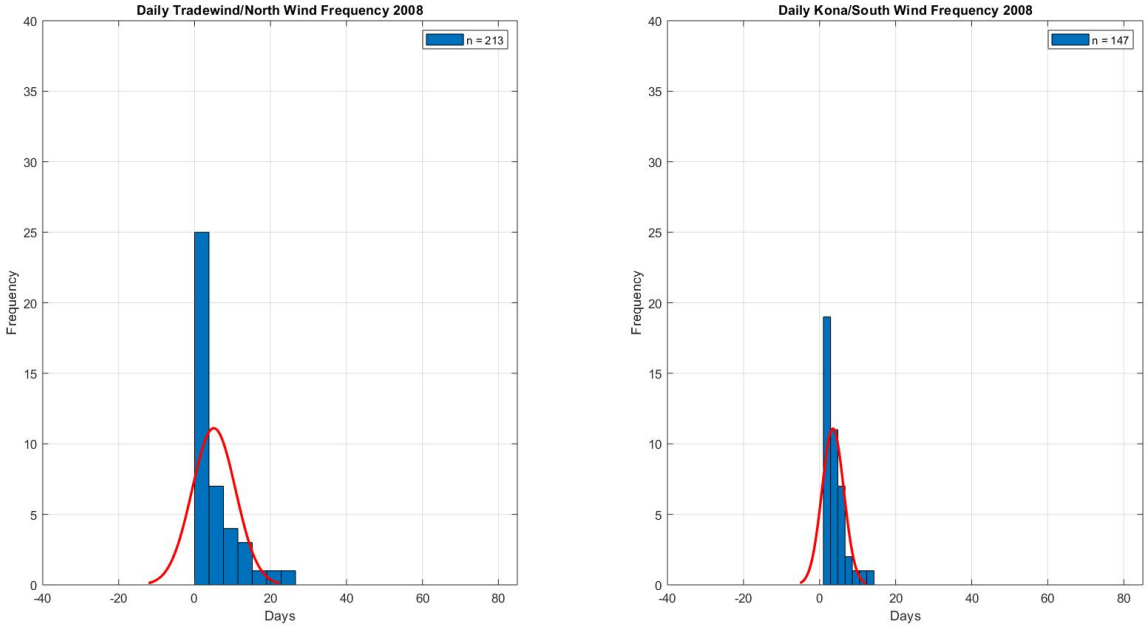

Figure 31. Daily Tradewind/north wind vs. Kona/south wind frequencies for year 2008 at the National Weather Service at the Honolulu International Airport.

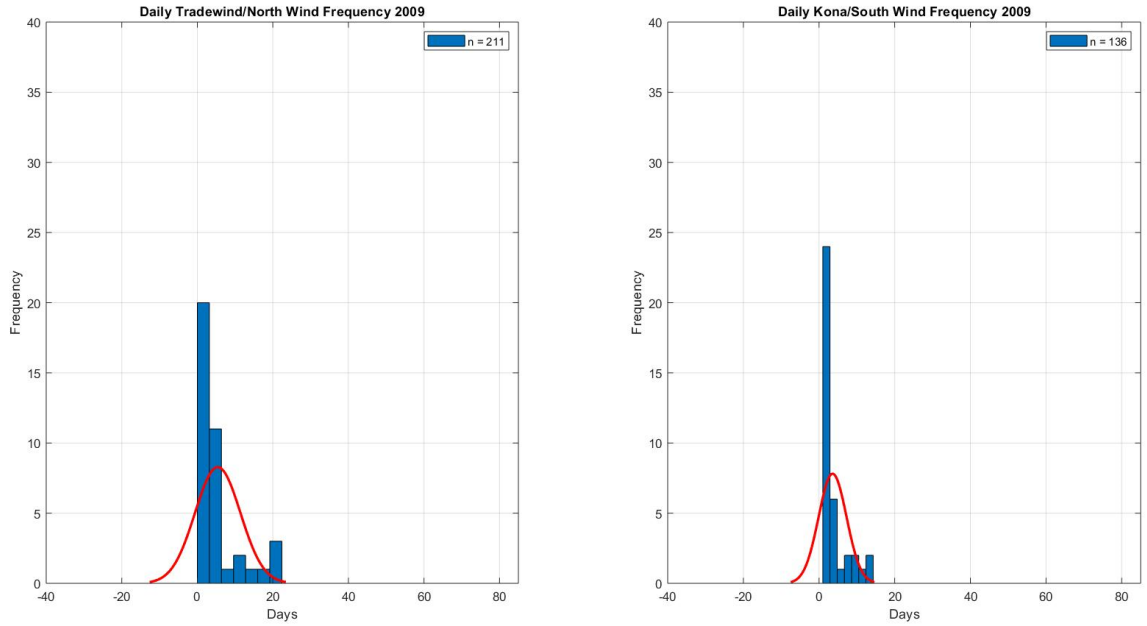

Figure 32. Daily Tradewind/north wind vs. Kona/south wind frequencies for year 2009 at the National Weather Service at the Honolulu International Airport.

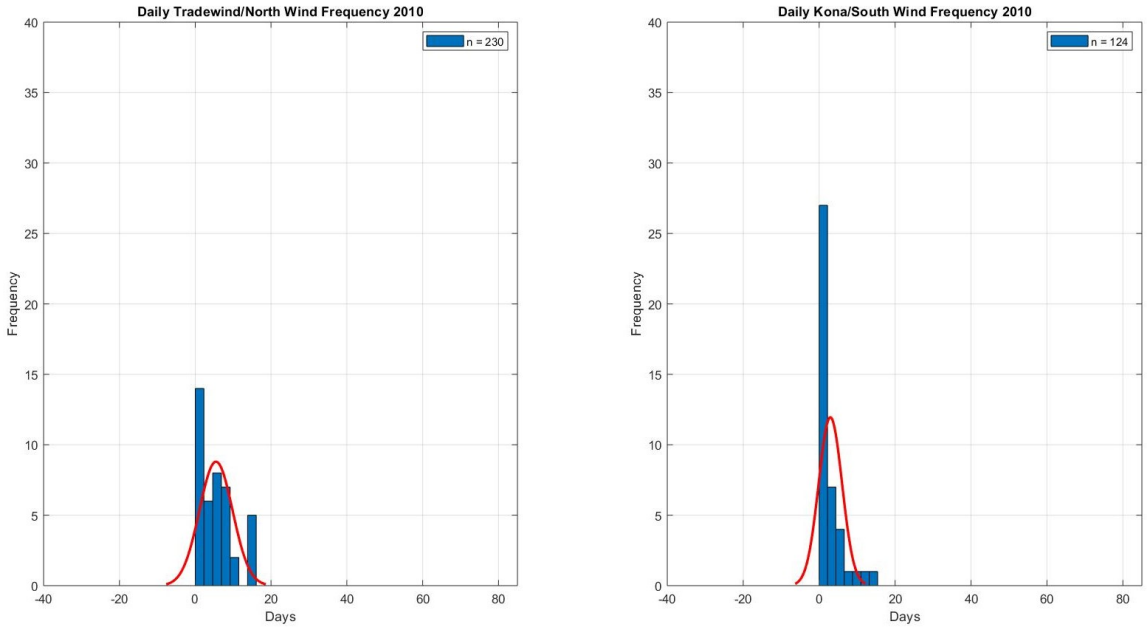

Figure 33. Daily Tradewind/north wind vs. Kona/south wind frequencies for year 2010 at the National Weather Service at the Honolulu International Airport.

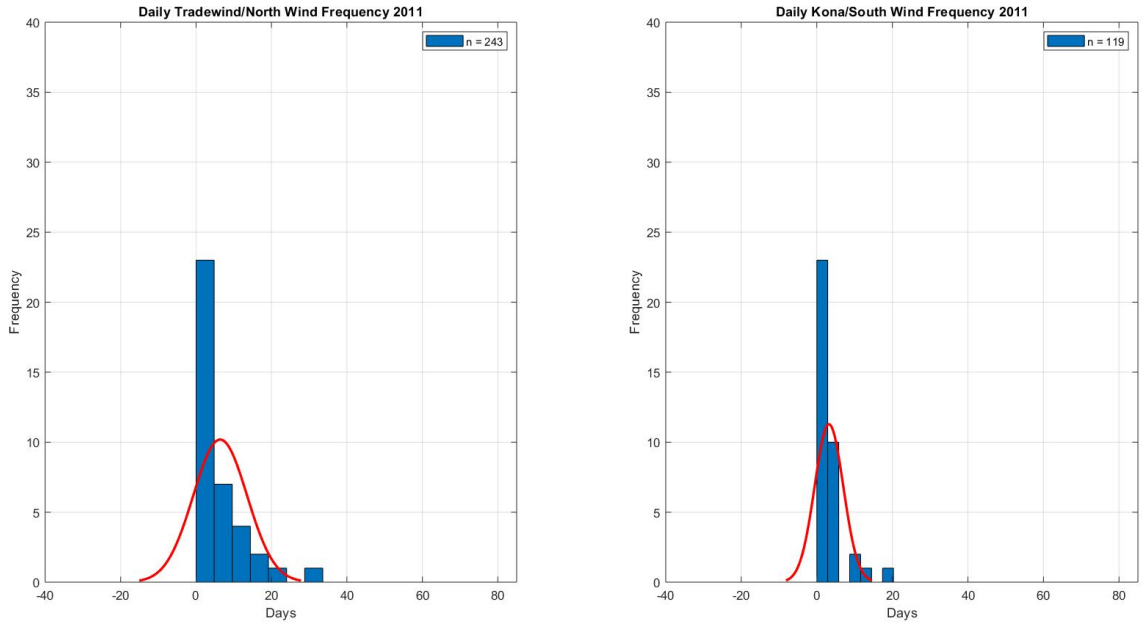

Figure 34. Daily Tradewind/north wind vs. Kona/south wind frequencies for year 2011 at the National Weather Service at the Honolulu International Airport.

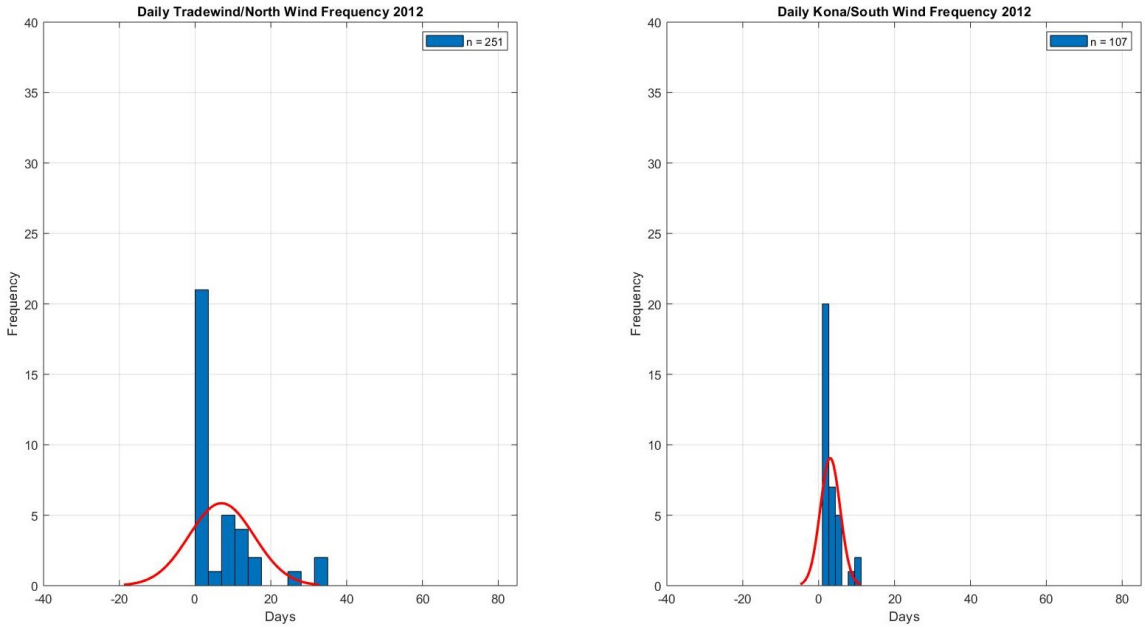

Figure 35. Daily Tradewind/north wind vs. Kona/south wind frequencies for year 2012 at the National Weather Service at the Honolulu International Airport.

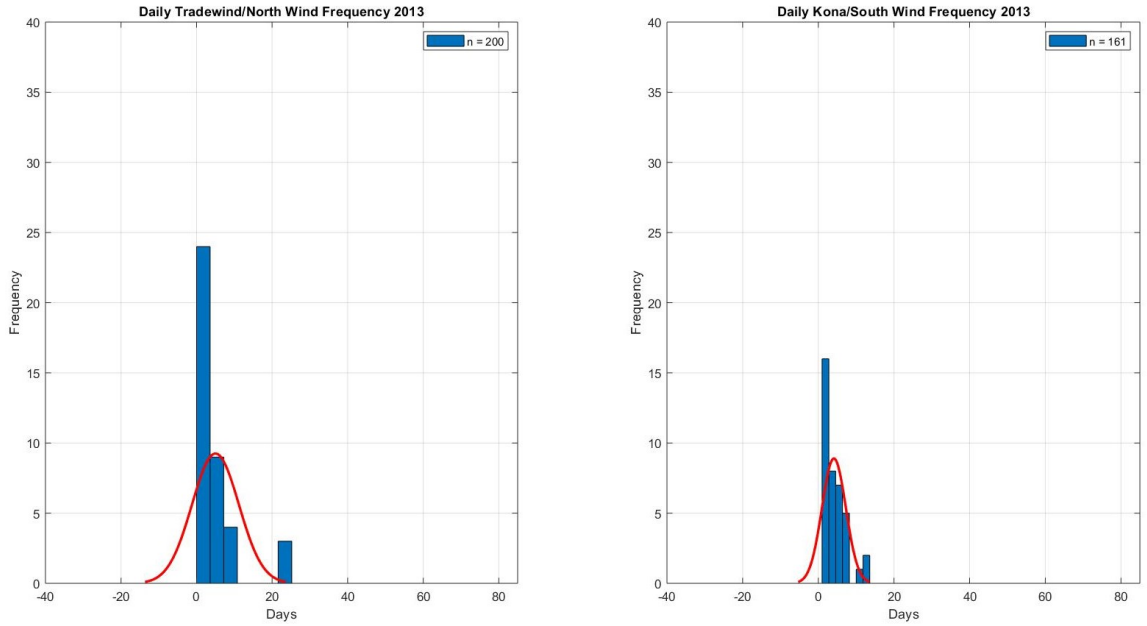

Figure 36. Daily Tradewind/north wind vs. Kona/south wind frequencies for year 2013 at the National Weather Service at the Honolulu International Airport.

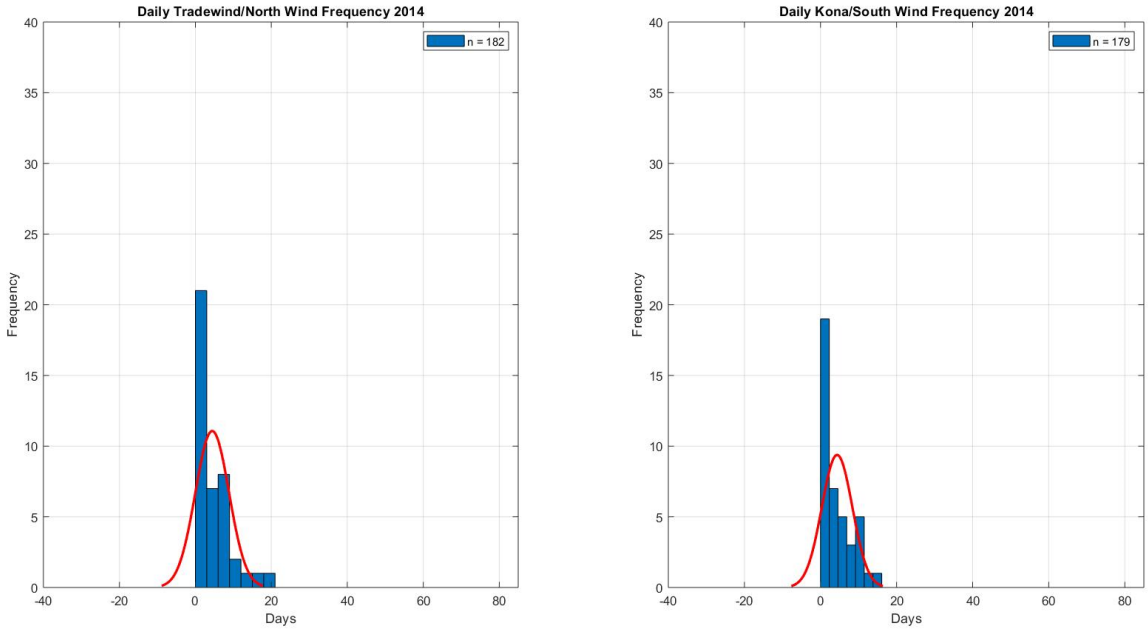

Figure 37. Daily Tradewind/north wind vs. Kona/south wind frequencies for year 2014 at the National Weather Service at the Honolulu International Airport.

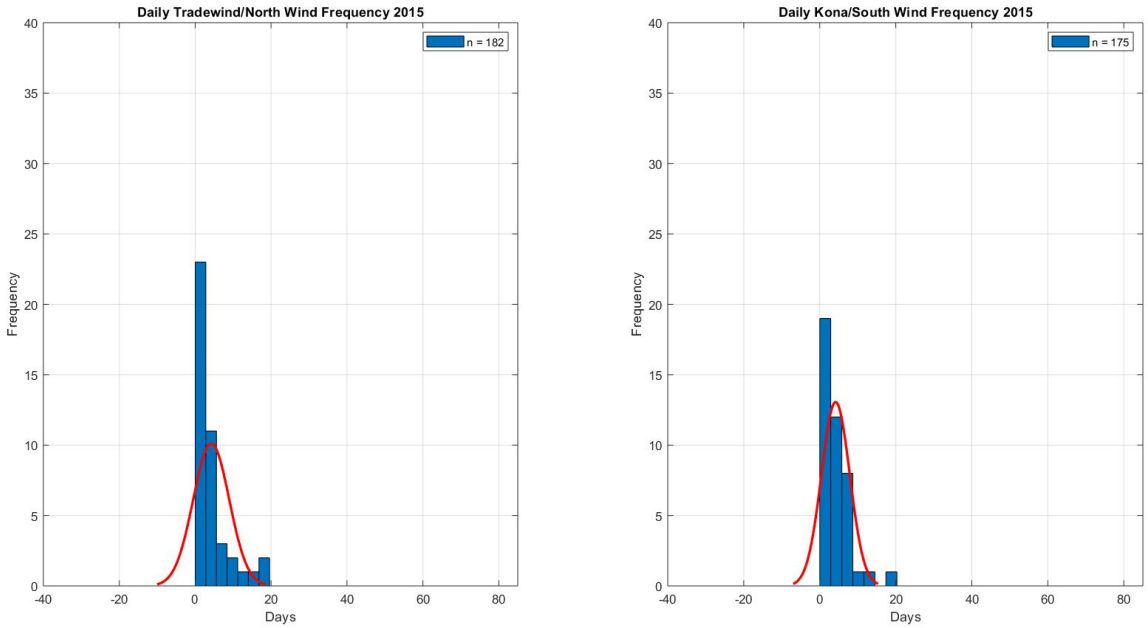

Figure 38. Daily Tradewind/north wind vs. Kona/south wind frequencies for year 2015 at the National Weather Service at the Honolulu International Airport.

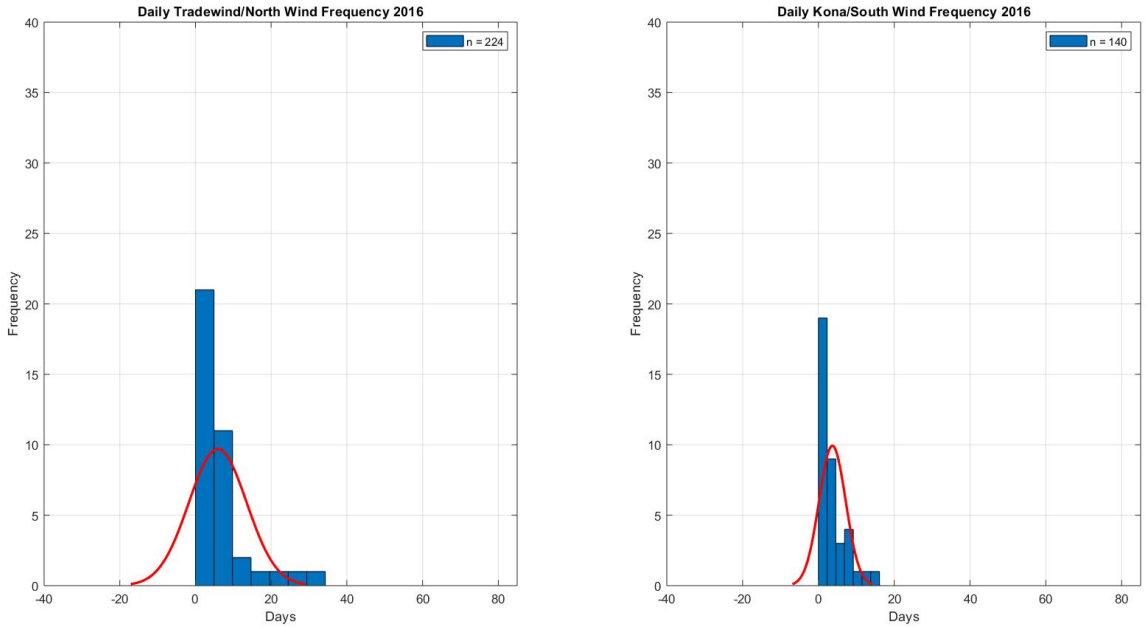

Figure 39. Daily Tradewind/north wind vs. Kona/south wind frequencies for year 2016 at the National Weather Service at the Honolulu International Airport.

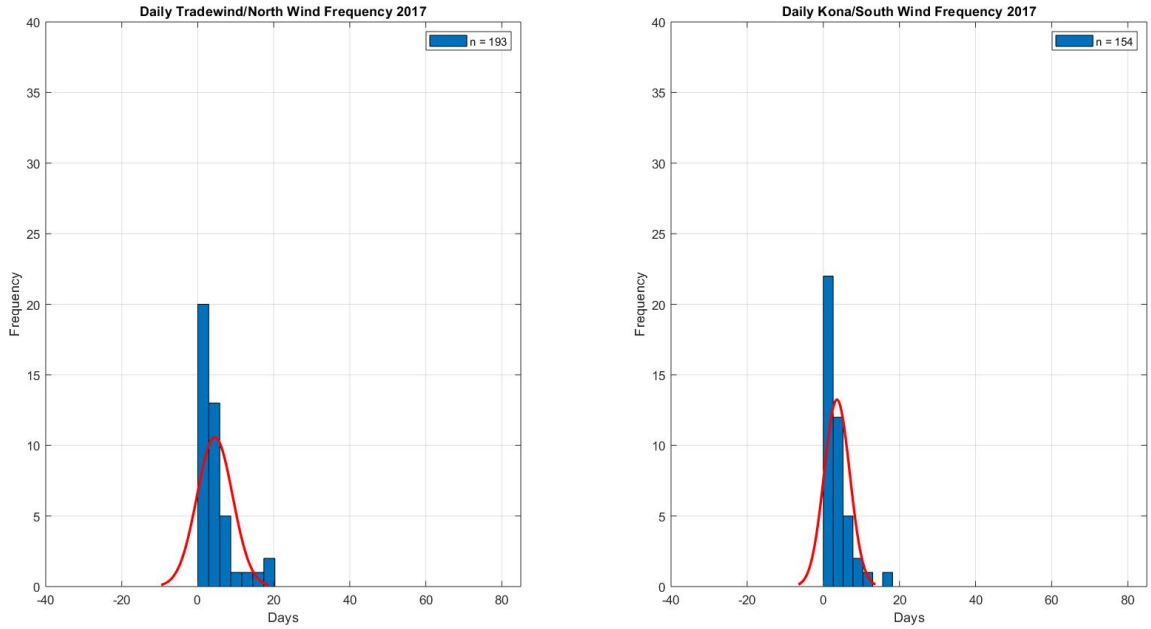

Figure 40. Daily Tradewind/north wind vs. Kona/south wind frequencies for year 2017 at the National Weather Service at the Honolulu International Airport.

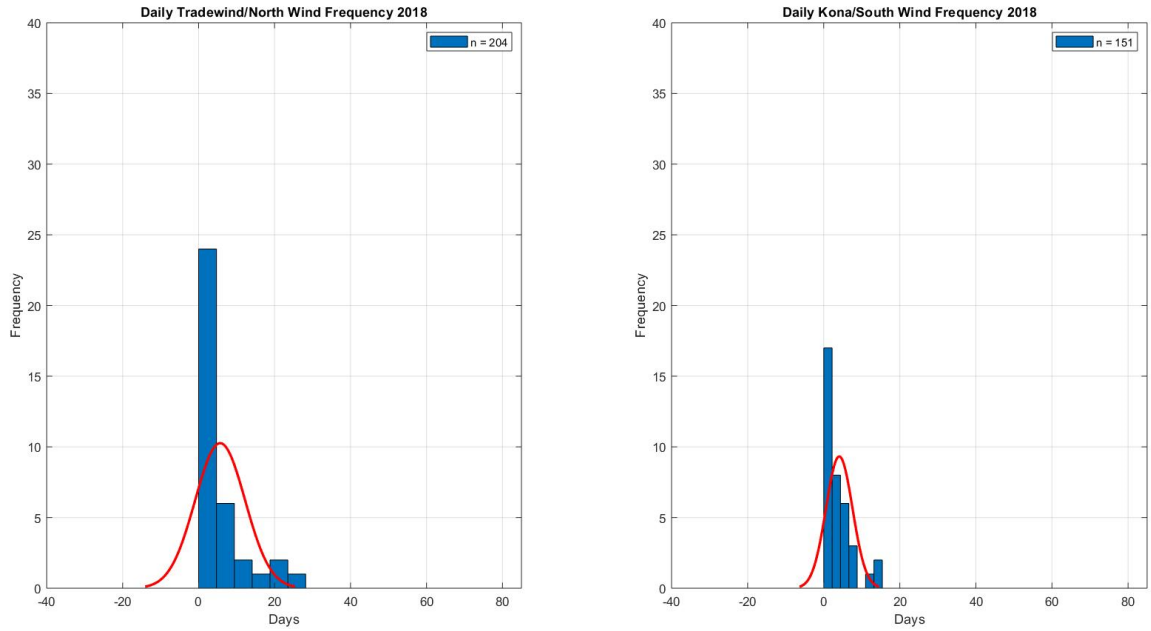

Figure 41. Daily Tradewind/north wind vs. Kona/south wind frequencies for year 2018 at the National Weather Service at the Honolulu International Airport.

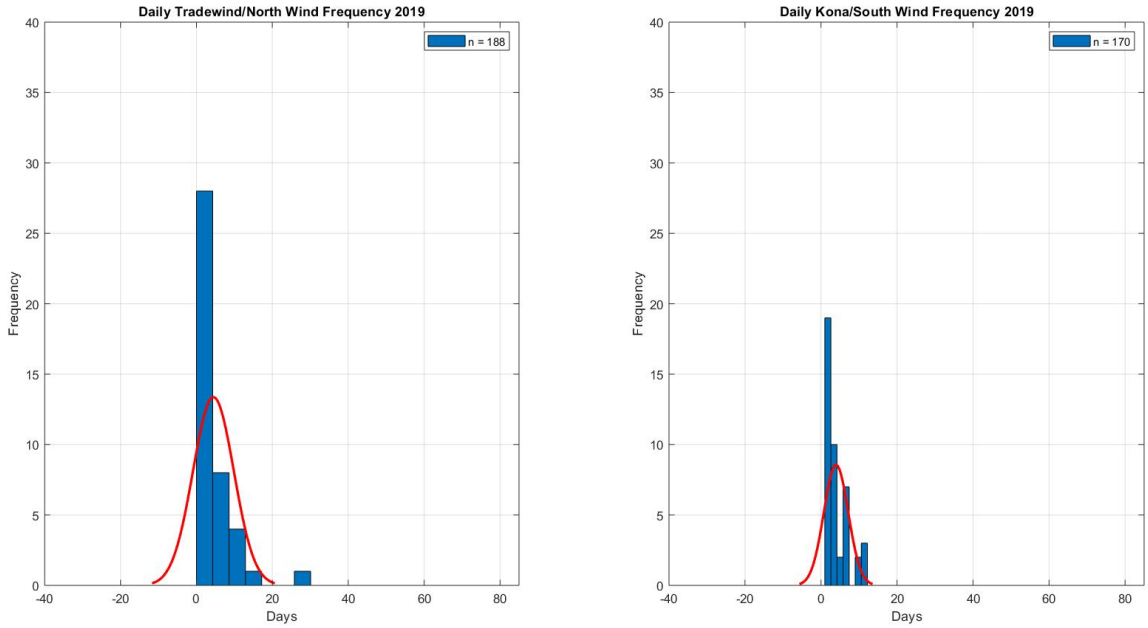

Figure 42. Daily Tradewind/north wind vs. Kona/south wind frequencies for year 2019 at the National Weather Service at the Honolulu International Airport.

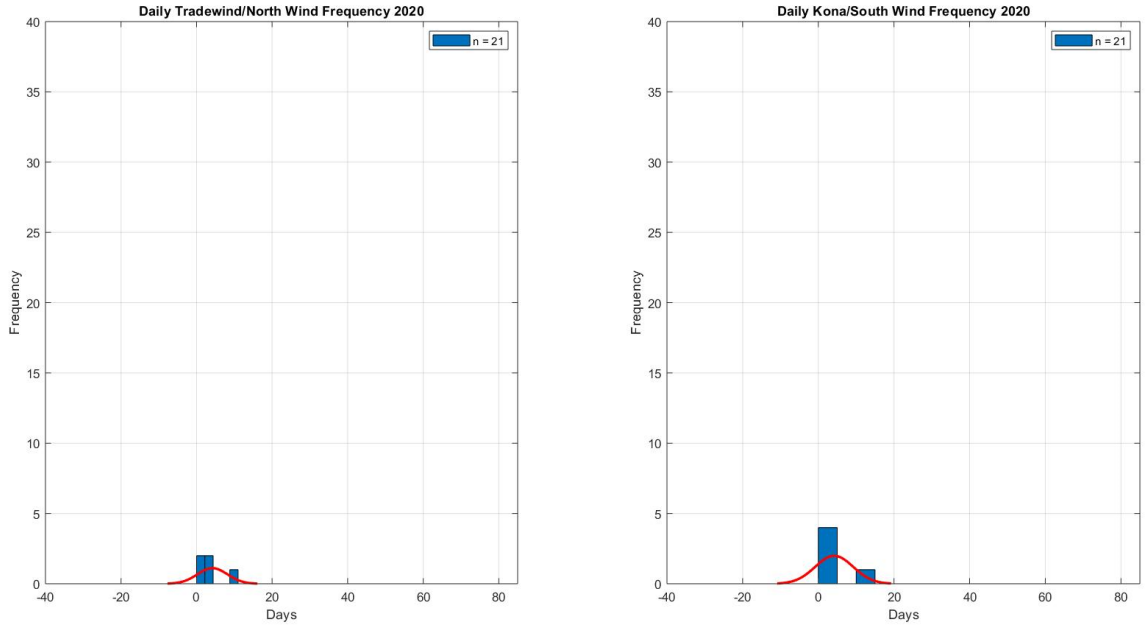

Figure 43. Daily Tradewind/north wind vs. Kona/south wind frequencies for year 2020 at the National Weather Service at the Honolulu International Airport.

4.0 Discussion

By using long-term, high-frequency data from the PacIOOS nearshore sensors, we can separate short-term fluctuations in temperature, salinity, pressure, chlorophyll and turbidity from long-term trends along the coastal waters of O‘ahu’s South Shore. These time-series data have given us a better understanding of the water quality conditions in both Mamala and Maunalua Bay, O‘ahu. In this contribution we focused on the inter-annual trends of each physical parameter these sensor packages gathered. By quantifying data, we can form connections between larger environmental processes, and attempt to establish causes for change over time; to attempt to determine whether trends are brought on by long-term environmental fluctuations, human-induced climate change, or a combination of the two.

4.1 Temperature

Over the course of our twelve-year sample collection, all four nearshore sensor monitoring sites measure an increase in near-surface temperature. All sites show strong daily, seasonal, and inter-annual variability. Daily temperature variability changes at each sensor site and may largely be due to season, solar insolation/cloud cover, geographic location, and physical surroundings. The seasonal cycle may vary from year-to-year due to large scale phenomena such as El Niño-Southern Oscillation (ENSO) and Pacific Decadal Oscillation (PDO) (Gove *et al.*, 2016). NS02 has more high frequency fluctuations than NS03, NS04 and NS10. With its placement at the mouth of the Ala Wai Canal attached to a floating dock, NS02 is influenced by both solar and tidal forcing, as well as freshwater outflow, creating a brackish water environment. NS02 shows large anomalous drops in temperature (below 23.0 ºC) throughout the duration of deployment. Most of these drops falling below 23.0 ºC occur in winter, or cooler months (November – April). All temperature drops below 23.0 ºC are accompanied with low salinity levels (1.7 – 35.4 PSU), indicating that they are the result of heavy rain events and freshwater outflow. NS02 may have the highest average daily temperature (26.8 ºC) among the four sensors due to its position in the Ala Wai Canal boat basin, away from open-ocean currents. NS02 is also unique in its vertical placement; this sensor is deployed on a floating dock closer to the surface than the other three sites (0.5 m), keeping a constant depth. This may account for increased effects of direct solar heating in the water and could also be a factor in the higher temperatures measured here.

NS03 is positioned vertically in the water column, attached to a mooring underneath the Atlantis Submarine Dock in Mamala Bay. Like NS02, this site receives direct freshwater input, but at a much lower level. The Hilton Hawaiian Village Lagoon is suspected to leech effluent from land, towards this site location, and is accompanied by long recovery times (~weeks) from low salinity levels after a rainfall event. NS03 does not receive direct solar heating and exhibits far less temperature fluctuation. Changes in temperature follow a strong seasonal pattern, with less daily variability. Temperatures below 23.0 ºC all occur in winter months. NS03 does not see the same deep daily drops accompanied with a decline in salinity from heavy rainfall events like NS02. The lack of consistent freshwater outflow near NS03 is likely an explanation for this tighter fit of temperatures. Because this fixed sensor sits deeper than NS02 at a depth of 1.0 m from the surface and is out of direct sunlight, its average daily temperature appears on the lower end of this study at 25.6 ºC. Along with the dock inhibiting direct solar heating of the water column, the structures may also constrain flow, potentially resulting in lower temperatures at some points of the tidal cycle.

Similar seasonal patterns are measured at NS04. All large drops in temperature are within winter months, and daily fluctuations appear within an average range. The location of this sensor is directly in front of the Waikiki Aquarium within Mamala bay and does not have any direct influence from freshwater. Its placement is horizontal in the water column 2.0 m below the surface. This sensor is fixed underneath an intake pipe with a much larger diameter than the CTD itself. This site is the furthest east within Mamala Bay and has a higher average daily temperature (25.9 ºC) than NS03. Although this sensor does not receive any direct sunlight, the intake pipe is likely not large enough to influence the average temperature in surrounding waters.

NS10 is positioned vertically in the water column, attached to a pylon, and is the only long-term monitoring station located in Maunalua Bay. This sensor has recorded strong seasonal oscillations in temperature, and the lowest amount of daily fluctuation. NS10 measures a broad temperature range of highs and lows. This occurrence may largely be due to its geographic location. Situated nearshore, between Portlock and Kuli‘ou‘ou Beach Park, NS10 is in a location with very dynamic coastal circulation. Water temperatures in Maunalua Bay ranged from 20.8 – 32.1 ºC, the greatest temperature difference in the study. This non-coherence of water temperatures may be the result of tidally driven interactions between deeper, cooler oceanic water and warmer nearshore waters (Storlazzi *et al*., 2010). During flood (rising) tide, the near-surface

currents predominantly push to the west and onshore, developing a counter-clockwise flow. During the ebb (dropping) tide, the near-surface currents create a clockwise circulation within the bay (Storlazzi *et al.*, 2010). This variability in direction and speed may account for the large temperature gradients, and the push of offshore waters nearshore may be the reason NS10 has the lowest average daily temperature of 25.5 ºC.

Although all the sensors are deployed along the south shore of O'ahu, within an 11-mile radius; on the short-term they display differences in the timing and range of diurnal heating. In the long-term however, the average daily temperatures align when compared with mean nearshore sea surface temperature, geospatial data sets (Selkoe, 2017). Increasing trends in daily average temperatures over the course of this study could be a result of local heating and or large-scale processes influencing regional scale conditions. However, when compared to both ENSO and PDO cycles discussed further below, there is no definite relationship found between temperature and these physical phases.

4.2 Salinity

All nearshore sensors measure water temperature and conductivity (S/m), from which salinity was calculated and measured in practical salinity units (PSU). Salinity is measured as a proxy for rainfall events, freshwater plumes and/or submarine groundwater discharge being advected past the instruments. All monitoring sites are considered inshore/nearshore, and therefore are subject to freshwater input. All nearshore sensors show a declining trend in near-surface salinity levels over the course of the twelve-year study. NS02 measured much higher frequency fluctuations than the other three sites, due to its placement at the mouth of the Ala Wai Canal. This site receives the most direct freshwater input, greatly influencing daily variability. The Ala Wai Canal is a channelization of three streams: Mānoa, Makiki and Pālolo. These streams receive large amounts of orographic rainfall daily, and thus is the main reason for the vast salinity range of NS02. Salinity measurements at the Hawai'i Yacht Club ranged from 1.7 – 35.4 PSU, with a daily average of 33.0 PSU and exhibits the highest standard deviation in the study of ± 2.0 PSU.

As previously stated, NS03 likely receives non-point source freshwater input form the Hilton Hawaiian Village Lagoon, however; the remaining nearshore sensors, NS04 and NS10 are neither adjacent, nor in close range of a point source, freshwater outlet. This becomes apparent when analyzing plots and raw data. NS03 exhibits the lowest frequency in daily fluctuation of salinity, 28.2 – 35.5 PSU. This low frequency

can be explained by a lack of consistent freshwater input, and potentially lower levels of submarine groundwater discharge. Greater variability in salinity is shown during times of heavy precipitation, accompanied with prolonged periods of low salinity levels. The average salinity of this site is 34.0 PSU with a standard deviation of ± 0.6 PSU.

NS04, like NS03 shows a low frequency in fluctuation, 28.3 – 35.9 PSU. An absence of direct freshwater input, and a lower level of submarine ground water discharge explains this low variability. NS04 has an average daily salinity level of 35.0 PSU with a standard deviation of ± 0.4 PSU.

While NS10 is not in direct contact with a freshwater source, it exhibits the second largest range in salinity frequency, 12.3 – 35.7 PSU. The main cause of this range is from a large rain event affecting the area on March 6th, 2012. Aside from NS02 being out of the water during this time, NS03 and NS04 were taking samples and did not measure such a dramatic decrease in salinity. This shows that NS10 may be influenced by an unknown freshwater source or have greater impact of submarine groundwater discharge. Other than the March 6th, 2012 rain event, salinity levels at NS10 were relatively constant but do exhibit more daily variability than NS03 and NS04. This may be influenced by the dynamics of Maunalua Bay and the tidally driven circulation, as well as nearshore submarine groundwater discharge.

4.3 Chlorophyll

Two of the nearshore sensors, NS02 and NS10, utilize the ECO double-channel fluorometer's for the measurement of relative fluorescence, or chlorophyll *a*. For this study, only night-time chlorophyll *a* was analyzed to account for excess light during the day and nonphotochemical quenching (NPQ). NPQ is the process by which phytoplankton cells dissipate excess energy absorbed by photosynthetic pigments, protecting plants against photoinhibition (Horton *et al*., 1996; Huot and Babin, 2010). When exposed to excess light, phytoplankton cells halt the transfer of photon energy between light harvesting complexes and chlorophyll *a* molecules, diminishing the release of photo energy as fluorescence (Krause and Weis, 1991; Horton *et al*., 1996). This process of NPQ manifests as a reduction in measured chlorophyll *a* during the daytime hours. Because plants recover from photoinhibition in unquenched night-time observations, we have chosen to only report night-time (>= 18:00:00, <=06:00:00) chlorophyll *a*. This pigment indicates phytoplankton biomass, and fluctuations can occur with variances in nutrient levels in the water column.

An increase in near-surface chlorophyll *a* was recorded at NS02, measuring higher frequency fluctuations in chlorophyll *a*, more often. Like temperature and salinity measurements at this site, location plays a large role in measured samples. With the Ala Wai Canal feeding into the Hawai‘i Yacht Club harbor, high levels of organic and inorganic nutrient input occur. Comparing salinity with night-time chlorophyll *a* at NS02 reveals that chlorophyll *a* peaks on the same timescale as salinity, suggesting relatively zero lag between a large rain event and an influx of phytoplankton. This nutrient level increases the level of phytoplankton biomass (Örnólfsdóttir, 2004), giving an average chlorophyll *a* reading of 2.8 µg/L.

NS10 experiences a lot of boat traffic, as it is adjacent to a channel, harbor and launch ramp facility, and is a susceptible to road runoff during heavy rain events, which can introduce large amounts of nutrients in a short period of time. This site does show an increase of chlorophyll *a* over the course of the study, but at a lower level than NS02. NS10 has an average chlorophyll *a* reading of 1.1 µg/L. With high levels of circulation, the nutrient influx into Maunalua Bay likely disperses at a quicker rate than at the Hawai‘i Yacht Club site in Mamala Bay.

Both sensors show some negative values in chlorophyll *a* measurements. This is caused by the calibration of the ECO Fluorometer sensor package, and the sensors dark count. The dark count rate is the average rate of registered counts without any incident light, determining the minimum count rate at which the signal is dominantly caused by real photons. The dark count is measured in volts or counts of the sensor in clean water with black tape over the detector. When utilized in the field, if a measurement falls below the calibrated dark count, values will be negative.

4.4 Turbidity

As previously mentioned, NS02 and NS10 are the only two sites that utilize the ECO double-channel fluorometers and can measure light attenuation, or turbidity. Turbidity is a measure of the degree to which water loses its transparency due to solids suspended in the water column. The higher the solids in the water, the murkier or more turbid the site. Like, chlorophyll *a*, phytoplankton can cause turbidity, as well as sediments from erosion, the resuspension of sediments, waste discharge, algal growth, and runoff. Turbid waters can be caused by human activities or natural events and create unsightly and dangerous environments. Both NS02 and NS10 measure turbidity in Nephelometric Turbidity Units (NTU). Due to manufacturer

calibration settings of their ECO fluorometer's, these two sites are not on similar ranges (the maximum measured turbidity levels were set to different values from instillation till present), however, relative trends can be compared.

NS02 was fitted with an ECO with maximum measurement capabilities of 100 NTU. This site has the highest daily turbidity value at 97.2 NTU, and with an average value of 2.06 NTU. Turbidity readings at NS02 are unique, as this sites sensor is closest to the surface (0.5 m) and the furthest from the bottom (6.0 m). Because it is so far from the bottom, the turbidity values are likely not caused by the resuspension of sediment from the floor (with the exception of the 2011 Tōhoku earthquake and tsunami), rather they may be caused by phytoplankton, waste discharge, erosional sediments, and algal growth. Similar to night-time chlorophyll *a*, we see turbidity values and salinity on the same timescale, suggesting relatively zero lag between a large rain event and increased turbidity.

NS10 was fitted with an ECO with maximum measurement capabilities of 25 NTU. This site depicts a much lower, maximum turbidity value of 24.8 NTU and has an average value of 7 NTU. This sensor is nearly at the seafloor. NS10's seabed composition is largely made up of sand, silt, clay, mud, and gravel. Coarse sediment particles like larger grain sand and gravel have higher settling velocities than finer particles like silt, clay, and mud. These particles with slow settling rates are susceptible to resuspension relative to tidal forcing's, wave activity, and human activity, all leading to possible increased turbidity readings (Swanson, 2009). Changing out NS10's lower calibrated ECO for a higher calibrated one would bear interesting results for future studies. Time-series data for both sites illustrates positive trends in turbidity over the period of study.

Both sensors show some negative values in turbidity measurements. Similar to chlorophyll *a* measurements as described in section 4.3, this is caused by the calibration of the ECO Fluorometer sensor package, and the sensors dark count. When utilized in the field, if a measurement falls below the calibrated dark count, values will be negative.

4.5 Pressure

Again, while three of the four nearshore sensors measure pressure data, NS04 at the Waikiki Aquarium was the only site analyzed. This location has the only mooring, which allows for horizontal placement of the senor, permitting precise re-deployment at a specific depth. While complex, pressure (m) and depth are directly related; the amount of pressure being exerted on the sensors pressure gauge can be used to determine the depth of the reading. Daily changes in pressure are dominated by sea-level changes due to Hawai‘i’s mixed, semi-diurnal tides, resulting in two high tides of different height and two low tides of different height each day. The pressure data will reflect this frequency change in these tidal intervals. Time-series data may capture fluctuations in seafloor topography, and changes in sea level caused by large physical phenomenon such as ENSO and PDO events, and human induced sea level rise through climate change and increased sea-surface temperatures (SST).

NS04 exhibits a high daily pressure of 2.9 m and a low of 1.2 m, with a site average pressure reading of 1.9 m. Throughout the twelve-year measurement history, there is an increasing trend in overall pressure (0.03 m), which can be caused by the above combination of factors. For the purpose of this study we are assuming the intake pipe has been immovable since the initial deployment of this sensor, thus, it is possible that this increasing trend is due to general sea-level rise. Looking at larger scale, physical events including ENSO and PDO discussed below, there do not appear to be any definite trends between the monthly averaged pressure fluctuation (Figure 13.) and the change between El Niño and La Niña episodes, nor does there appear to be a definite relationship with warm and cool anomalies in PDO cycles.

4.6 El Niño-Southern Oscillation (ENSO)

The El Niño-Southern Oscillation (ENSO) is an irregular, large-scale ocean-atmosphere climate phenomenon (Neelin *et al*., 1998), and is the most prominent year-to-year climate variation on Earth (McPhaden *et al*., 2006). Broken down into two phases, El Niño represents the warm phase and La Niña represents the cool phase of the ENSO cycle. El Niño is characterized by a weakening of the trade winds across much of the Pacific, in turn, a warming of ocean temperatures in the Equatorial Pacific. Duration of these warm phases typically last between 9 – 15 months (Gove *et al*., 2016). La Niña periods are characterized by stronger than normal trade winds, pushing surface waters, and creating anomalously cool ocean

temperatures. On average, La Niña phases last longer, approximately 1 – 3 years, and are considered a less extreme anomaly than El Niño (Gove *et al.*, 2016). A multivariate ENSO index (Figure 44) indicates the strength of ENSO cycles: positive represents El Niño conditions and negative values represent La Niña conditions. ENSO oscillates between El Niño and La Niña, and over the past half-century, this fluctuation has been rather consistent. However, since 1976, there has been a shift towards increased prevalence of and strength in El Niño conditions (Gove *et al.*, 2016). Across the duration of this study, 2013 - 2016 was a very strong El Niño.

This large-scale physical phenomenon impacts local climate and oceanographic conditions, such as lower than average, or higher than average precipitation, increased swell activity, and higher observed SST; all of which can largely influence the physical parameters recorded by the sensor packages. Temperature and pressure time-series from the nearshore sensors were compared against ENSO cycles in this study, and neither showed correlations. Because the oscillation period changes at a relatively low frequency (4 – 6 years) (An and Wang, 2000), our dataset would need to extend for multiple decades, two at minimum. Thus, it appears that the temporal variability is primarily driven by local influences.

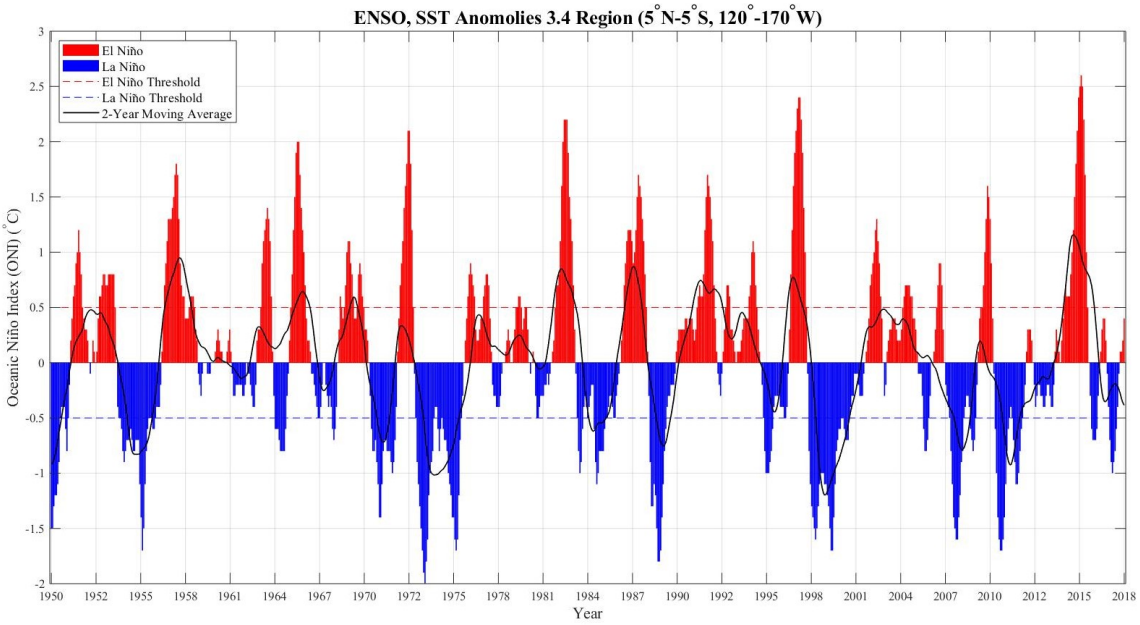

Figure 44. Multivariate ENSO Index from 1950 to 2018. Positive (red) values represent El Niño, warm conditions and negative (blue) represents La Niña, cool conditions. Black line represents two-year moving average, and dotted lines represent threshold of > or < 0.5ºC.

4.7 Pacific Decadal Oscillation

The Pacific Decadal Oscillation (PDO) can be described as a long-lived El Niño-like pattern of Pacific climate variability (Zhang *et al*., 1997). Like ENSO, the extreme phases of PDO are classified as being either warm or cool phases, defined by ocean temperature anomalies (Gove *et al*., 2016). When SSTs are anomalously warm in the tropical pacific, and when sea level pressure are below average, the PDO has a positive value and is indicated as a warm phase (Mantua and Hare, 2002).

This physical phenomenon is longer lived than ENSO, and tends to stand for multiple decades with short-lived, intermittent reversals (Gove *et al*., 2016). Over the past two decades, the PDO was predominately in a cool phase, until more recently in 2015, the PDO switched to warm phase (Figure 45). As previously stated, this large-scale phenomenon can have a large impact on local climate and oceanographic conditions, and when coupled with an El Niño period, accompanying issues may be exacerbated. Because PDO experiences longer scale fluctuations (20 – 30 years) (Mantua and Hare, 2002), making connections between temperature and pressure data from this study has great room for error because of the length of our dataset, and does not provide a comparison. To correlate the nearshore sensor data to PDO data, we would need to continue sampling for a dataset of 50+ years.

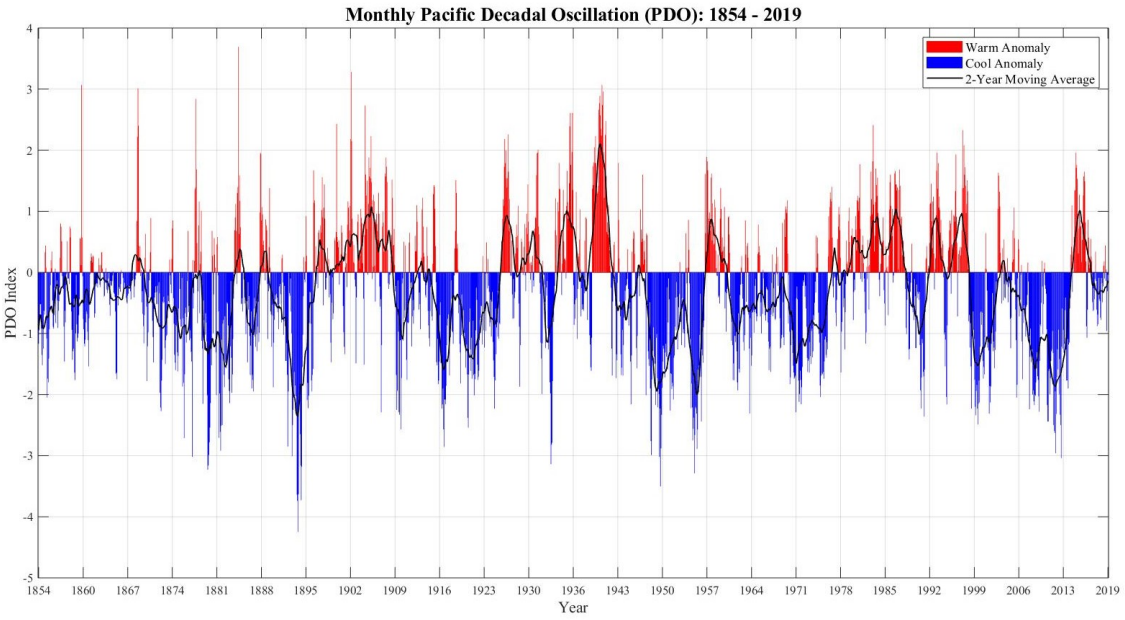

Figure 45. Pacific Decadal Oscillation Index from 1854 to present. Positive (red) values represent Warm Anomaly conditions and negative (blue) values represent Cool Anomaly conditions. Black line is a two-year moving average.

4.8 Rainfall

Tracking the status and trends in rainfall patterns is important for many resource management issues. Changes in rainfall patterns over time can determine the amount and the intensity of ground water and surface water transport in coastal environments, which may influence nearshore salinity and temperature patterns, as well as suspended sediment and nutrient concentrations (Gove *et al*., 2016).

The Hawaiian Islands have massively diverse rainfall patterns, and O‘ahu is no exception. Persistent trade winds, mountainous terrain, and diel heating and cooling on land, generates orographic uplift. Resulting clouds and rainfall produced by this uplift leads to dramatic differences in mean rainfall over short distances across the island (Giambelluca *et al*., 2013).

Rain data was taken from the United States Geological Survey (USGS) Moanalua rain gauge from 2008 over the course of this study. This historic record of rainfall in the region exhibited somewhat consistent seasonal and inter-annual patterns. Long-term data shows neither an increase nor decrease in rainfall from 2007 – 2019. The Moanalua rain gauge was chosen for this study due to its similar installment timeframe, however its distant proximity may contribute inadequate data for our four nearshore sensor locations.

4.9 Wind

The trade wind pattern over the Pacific Ocean is one of the largest and the most consistent wind fields in the world (Wyrtki and Meyers, 1976). This large-scale wind pattern is present in Hawai‘i from 85 – 95% of our summers, and from 50 – 80% of our winters (Sanderson, 1993), and may see changes in frequency due to the natural variability in physical patterns such as ENSO and PDO cycles. The persistent northeast trade winds are important to our islands, as they influence wave height, cloud formation, precipitation, and nearshore circulation over specific areas of the region (Garza *et al*., 2012). When trades from the northeast or east-northeast direction fail, and shift to a south wind the air can become dormant; developing unpleasant weather, light winds, high humidity, changes in rainfall patterns and distribution, and shifts in nearshore circulation (Schroeder, 1981). Tracking these changes in Hawai‘i’s wind patterns over the course of this collaboration is important to understand the frequency and intensity of the shifts between prevailing trade winds and southern Kona winds.

Data taken from the National Weather Service Honolulu International Airport wind station from 2000 to present was utilized over the course of this study. This historic record of wind for the region exhibits changes in directional frequency over time. While trade winds remain the dominant pattern over the records course (n = 4404), the overall frequency of trades have decreased overtime, and subsequently, the frequency of Kona winds have increased.

4.10 Climate Change

The atmospheric concentration of carbon dioxide (CO_2) has been steadily increasing since the Industrial Revolution, and despite efforts, will continue to increase for the foreseeable future (Xie *et al*., 2010). Our human influence on the climate system is clear, and anthropogenic emissions of greenhouse gases have had widespread impacts on natural systems (IPCC, 2014). The warming of the climate is indisputable, and since the 1950's, many of the observed changes are unprecedented over decades to millennia, irreversibly disturbing Earth's atmosphere and oceans (IPCC, 2014).

The globally combined land and ocean surface temperature data show an averaged warming of 0.85 ºC over the period of 1880 to 2012 (IPCC, 2014). Consistent with a global trend, Hawai'i temperature experienced an upward trend: 0.04 ºC decade^{-1} from 1919 – 2006, and 0.16 ºC decade^{-1} for the past 30 years (Giambelluca *et al*., 2008). Ocean warming dominates this increase in stored energy in the climate system, accounting for more than 90%, as opposed to 1% stored by the atmosphere (IPCC, 2014). Ocean warming is largest near the surface (75 m) and has warmed by 0.11 ºC decade^{-1} from 1971 to 2010 (IPCC, 2014).

This coupled, atmospheric and oceanic warming is expected to bring extreme events in temperature, changes in precipitation, sea level rise and more. Excess energy from the generation of greenhouse gas emissions is absorbed into the ocean as heat. Rising temperatures affect marine species and ecosystems, salinity levels, sea level, and the fundamental benefits which humans derive from the ocean. As oceans warm, evaporation increases. It is likely that regions of high surface salinity, where evaporation dominates, have, and will continue to become more saline, while regions of lower salinities, where precipitation dominates, are becoming fresher (IPCC, 2014). The global mean sea level has risen by 0.19 m from 1901 – 2010, likely rising at a rate of 1.7 mm yr^{-1} between 1901 and 2010, and 3.2 mm yr^{-1} between 1993 and 2010 (IPCC, 2014). Over the past century, sea level at the Honolulu Harbor tide gauge, the longest on record throughout Pacific islands,

has risen at 1.4 ± 0.3 mm yr^{-1} (Caccamise II *et al*., 2005). It is said with high confidence that the loss of glacial ice and thermal expansion from ocean warming explains 75% of the observed global mean sea level rise (IPCC, 2014).

On our local scale, PacIOOS nearshore sensors have measured an averaged increase in temperature (1.06 ºC) and an averaged decrease in salinity (-1.07 PSU), at all monitoring stations, as well as an increase in pressure at NS04 (0.03 m). The increase in temperature may coincide with the shift in overall frequency of trade winds in Hawai‘i, which have decreased, as the frequency of Kona winds have increased over time. The measured decrease in salinity does not correspond with the rainfall trends from the Moanalua rain gauge, however, rain data in closer proximity to the nearshore sensors should be examined and evaluated. Lastly, pressure data measured over our course of study shows greater sea level rise than in comparable, long-term studies. These differences in values when measured across similar research suggests that we need more time to evaluate these trends. Accumulating evidence recommends studies relative to global climate measure conditions over a thirty-year period or longer (McMichael *et at*., 2016). While data for this collaboration has been measured over 10 – 12 years; seemingly short-term in comparison to global climate change data, our results imply that, given more time, climate change may act as an explanation towards our findings.

5.0 Conclusion

More than 3.6 million measurements of oceanographic data and the resulting water-column properties have been made over the course of this twelve-year study. Key findings from these measurements and analyses include the following.

1. Due to the wide range of water quality parameters recorded and observed throughout the deployment of these nearshore sensors, we were able to sufficiently characterize oceanographic conditions along O‘ahu’s South Shore. Comparing the sensors physical data against a combination of atmospheric and oceanic conditions aimed to explain trends in nearshore sensor data over the study period, showing that local variability deviated from expected outcomes.
2. Overall, near-surface temperature at all four monitoring stations shows an upward trend. Daily temperature fluctuation changes at each sensor site and may largely be due to season, solar insolation/cloud cover, geographic location, and their physical surroundings and placement. All sites show strong seasonal and daily variability. Seasonal and inter-annual cycles were compared against large scale phenomena such as ENSO and PDO events, however, these data do not demonstrate conclusive correlations, as our dataset does not extend for a long enough period. NS02 at the Hawai‘i Yacht Club in Mamala Bay exhibits the highest average temperature (26.8 ºC) and the most high frequency fluctuations among the four sensors.
3. All nearshore sensor sites show a declining trend in near-surface salinity levels, and changes in salinity are largely due to daily variability from rainfall events and other freshwater inputs. NS02 depicts much higher frequency fluctuations in salinity, and the lowest average salinity level. This is most likely explained by its placement in the Ala Wai Canal, providing direct freshwater input. Rainfall data was measured against gathered salinity data. The Moanalua Rain Gauge was chosen due to its similar installment timeframe, however, its distant proximity proved to be unreliable when comparing data.
4. Two nearshore sensors, NS02 and NS10, are capable of measuring chlorophyll *a*. Only night-time chlorophyll *a* was measured for both sites (>= 18:00:00, <= 06:00:00). Analysis concludes positive trends in measured values overtime. NS02 shows higher frequency fluctuations, with an

average reading of 2.8 µg/L. NS10 has an average chlorophyll *a* reading of 1.1 µg/L. This gap in measured values may best be interpreted as a difference in geographic location, placement of sensors, and environmental influences.

5. Similarly, NS02 and NS10 were the only two sites in this study capable of measuring turbidity. Both nearshore sites illustrate positive trends in turbidity from instillation to present. However, due to manufacturer calibration settings of each monitoring stations ECO fluorometer, these two sites are incomparable, and only NS02 was used. NS02 exhibits an average turbidity value of 2.06 NTU.
6. NS04 was the only site which pressure was analyzed. This location utilizes a fixed horizontal mooring, which allows for precise re-deployment at a specific depth. NS04 shows a high daily pressure of 2.9 m, a low of 1.2 m, and a site average of 1.9 m. This nearshore station measured an increasing trend in pressure (0.03 m) over its decade of measurement history. It is possible that this trend may be a product of local sea-level rise, however, data collection should reflect a thirty-year period to make this statistically relevant.
7. Large, global-scale physical phenomenon's such as ENSO and PDO were investigated and compared against the nearshore sensor data. These cycles can impact local climate and oceanographic conditions, which can influence the sensors recorded data. Neither ENSO nor PDO showed significant correlations, as neither provided a reliable comparison due to the length of our dataset, but we expect that with continued study and a resulting longer-term data record, our findings will more closely correlate with research conducted on these global cycles.
8. The Moanalua rain gauge chosen for this study was too distant for adequate comparisons against our four nearshore sensor locations. Future work will utilize stream gauge data from the three streams (Mānoa, Pālolo and Makiki) which feed into the Ala Wai Canal.
9. The historic record of winds taken from the Honolulu International Airport exhibits changes in directional frequency from 2000 – 2020. Trade winds remain the dominant pattern, but the overall frequency of trades has decreased overtime, while the frequency of Kona winds has increased. This shift can change near-surface circulation patterns, affecting measurements taken by the nearshore sensors.

10. Although data from this study has only been measured over 10 – 12 years, our results show statistically relevant trends in physical measurements taken by our nearshore sensors. Evidence suggests that studies relative to global climate measure conditions over a thirty-year period or longer (McMichael *et at*., 2016). Thus, we need to collect more data over a longer period. An additional twenty years of samples taken from our four nearshore monitoring stations may provide evidence necessary to portray the degree of which global climate change is impacting the island.

Data from the PacIOOS nearshore sensors provides information on long-term water quality trends along the coastal waters of Mamala and Maunalua Bay, O‘ahu. These complex parameters have been observed for over a decade in attempts to better understand the implications and processes which both humans and nature impose on coastal water quality. The quantification of spatial and temporal physical trends in the referenced parameters allow insight into the past, present, and future state of Hawai‘i’s coastal water conditions. While the sample period of this collaboration is comparatively short against a global timescale, our results do tell a story. More than 3.6 million measurements of oceanographic data and the resulting water-column properties have been made over the course of this research. The coastal environment and water quality conditions along the south shore of O‘ahu are changing, and we have found statistically significant trends across all sites. The continuation of deployment of the PacIOOS nearshore sensors is imperative for the comparison of local, Hawai‘i water quality and global coastal environments. Further investigation and extension of this research group would be beneficial in establishing and exploring connections between local trends and the discussed long-term environmental processes and patterns. Ultimately, encouraging action in Hawai‘i’s efforts to adapt, plan, and implement policies to protect our coasts and communities against the effects of climate change on oceans and sea levels.

References

An, Soon-Il, and Bin Wang. "Interdecadal change of the structure of the ENSO mode and its impact on the ENSO frequency." *Journal of Climate* 13.12 (2000): 2044-2055.

Caccamise, Dana J., et al. "Sea level rise at Honolulu and Hilo, Hawaii: GPS estimates of differential land motion." *Geophysical Research Letters* 32.3 (2005).

De Carlo, E. H., Hoover, D. J., Young, C. W., Hoover, R. S., & Mackenzie, F. T. (2007). Impact of storm runoff from tropical watersheds on coastal water quality and productivity. *Applied Geochemistry*, *22*(8), 1777-1797.

Garza, Jessica A., et al. "Changes of the prevailing trade winds over the islands of Hawaii and the North Pacific." *Journal of Geophysical Research: Atmospheres* 117.D11 (2012).

Giambelluca, Thomas W., Henry F. Diaz, and Mark SA Luke. "Secular temperature changes in Hawai‘i." *Geophysical Research Letters* 35.12 (2008).

Giambelluca, T. W., Chen, Q., Frazier, A. G., Price, J. P., Chen, Y. L., Chu, P. S., ... & Delparte, D. M. (2013). Online rainfall atlas of Hawai‘i. *Bulletin of the American Meteorological Society*, *94*(3), 313-316.

Gove, J. M., Polovina, J. J., Walsh, W. A., Heenan, A., Williams, I. D., Wedding, L. M., ... & Heron, S. F. (2016). West Hawai'i integrated ecosystem assessment: ecosystem trends and status report.

Horton, P., Ruban, A. V., & Walters, R. G. (1996). Regulation of light harvesting in green plants. *Annual review of plant biology*, *47*(1), 655-684.

Huot, Y., & Babin, M. (2010). Overview of fluorescence protocols: theory, basic concepts, and practice. In *Chlorophyll a fluorescence in aquatic sciences: Methods and applications* (pp. 31-74). Springer, Dordrecht.

Krause, G. H., & Weis, E. (1991). Chlorophyll fluorescence and photosynthesis: the basics. *Annual review of plant biology*, *42*(1), 313-349.

Mantua, N. J., & Hare, S. R. (2002). The Pacific decadal oscillation. *Journal of oceanography*, *58*(1), 35-44.

McPhaden, Michael J., Stephen E. Zebiak, and Michael H. Glantz. "ENSO as an integrating concept in earth science." *science* 314.5806 (2006): 1740-1745.

McMichael, A. J., Campbell-Lendrum, D., Kovats, S., Edwards, S., Wilkinson, P., Wilson, T., ... & Schlesinger, M. (2004). Global climate change.

Neelin, J. D., Battisti, D. S., Hirst, A. C., Jin, F. F., Wakata, Y., Yamagata, T., & Zebiak, S. E. (1998). ENSO theory. *Journal of Geophysical Research: Oceans*, *103*(C7), 14261-14290.

Oki, D. S., & Brasher, A. M. (2003). Environmental setting and the effects of natural and human-related factors on water quality and aquatic biota, Oahu, Hawaii (Vol. 3, No. 4156). *US Department of the Interior, US Geological Survey.*

Swanson, M. K. (2009). Variability In Suspended Solids Measured at the Kilo Nalu (Doctoral dissertation, *University of Hawai‘i*).

Örnólfsdóttir, E. B., Lumsden, S. E., & Pinckney, J. L. (2004). Phytoplankton community growth-rate response to nutrient pulses in a shallow turbid estuary, Galveston Bay, Texas. *Journal of plankton research*, *26*(3), 325-339.

Sanderson, Marie, ed. Prevailing trade winds: climate and weather in Hawaii. *University of Hawaii Press*, 1993.

Schroeder, Thomas A. "Characteristics of local winds in northwest Hawaii." *Journal of Applied Meteorology* 20.8 (1981): 874-881.

Storlazzi, C. D., Presto, K. M., Logan, J. B., & Field, M. E. (2010). Coastal circulation and sediment dynamics in Maunalua Bay, Oahu, Hawaii. *USGS Open-File Report, 1217*, 2010.

Wyrtki, Klaus, and Gary Meyers. "The trade wind field over the Pacific Ocean." *Journal of Applied Meteorology* 15.7 (1976): 698-704.

Xie, Shang-Ping, et al. "Global warming pattern formation: Sea surface temperature and rainfall." *Journal of Climate* 23.4 (2010): 966-986.

Zhang, Y., Wallace, J. M., & Battisti, D. S. (1997). ENSO-like interdecadal variability: 1900–93. *Journal of Climate*, *10* (5), 1004-1020